

Modifying Final Splits of Classification Tree for Fine-tuning Subpopulation Target in Policy Making

Lei Bill Wang¹ Zhenbang Jiao² Fangyi Wang²

Abstract

Policymakers often use Classification and Regression Trees (CART) to partition populations based on binary outcomes and target subpopulations whose probability of the binary event exceeds a threshold. However, classic CART and knowledge distillation method whose student model is a CART (referred to as KD-CART) do not minimize the misclassification risk associated with classifying the latent probabilities of these binary events. To reduce the misclassification risk, we propose two methods, Penalized Final Split (PFS) and Maximizing Distance Final Split (MDFS). PFS incorporates a tunable penalty into the standard CART splitting criterion function. MDFS maximizes a weighted sum of distances between node means and the threshold. It can point-identify the optimal split under the unique intersect latent probability assumption. In addition, we develop theoretical result for MDFS splitting rule estimation, which has zero asymptotic risk. Through extensive simulation studies, we demonstrate that these methods predominately outperform classic CART and KD-CART in terms of misclassification error. Furthermore, in our empirical evaluations, these methods provide deeper insights than the two baseline methods.

1. Introduction

Policymakers often use CART to partition a population based on a binary event $Y = 1$ and target a few subpopulations with a probability of $Y = 1$ higher than a threshold c when implementing a policy. We call such policy targeting problems Latent Probability Classification (LPC).¹ Here,

¹Department of Economics, Ohio State University, Columbus Ohio, USA ²Department of Statistics, Ohio State University, Columbus Ohio, USA. Correspondence to: Lei Bill Wang <wang.13945@osu.edu>.

¹Note that LPC is a generalization of classification based on minimizing “0-1 loss” (i.e. the misclassification rate of the ob-

we give three policymaking contexts that match LPC setup. For more examples in existing literature, see Appendix A.1.

Social assistance: Andini et al. (2018) uses CART to find subpopulations with a higher than 50% probability of being financially constrained and target these households with a tax credit program.

Forest fire: Sarkar et al. (2024) uses CART to determine which forest zone has a higher than 61% probability of forest fire to implement early warning systems.

College admission: Mashat et al. (2012) uses CART to find among all university applicants which subpopulation has more than 50% probability of getting accepted to filter out the “low-level candidates”.

The three examples use CART to divide the sample into many nodes, estimate the probability of $Y = 1$ for all nodes, and target those nodes with estimated probabilities higher than a given threshold c . For example, $c = 61\%$ in the forest fire example.

This approach, though intuitive, does not generate the binary splitting rule that minimizes the LPC misclassification risk of classifying whether $\mathbb{P}(Y = 1|X)$ is above or below c . We will formally define the LPC misclassification risk in Section 2 and explain its policy significance in Section 5. Here, we provide a toy example in Figure 1a to illustrate the limitation of using CART for an LPC problem.

Suppose the latent probability of a binary event $Y = 1$ is a sinusoidal function of an observable variable X , i.e.,

$$\mathbb{P}(Y = 1|X) = \frac{\sin(2\pi X) + 1}{2} \text{ where } X \sim \text{Unif}[0, 1].$$

If we set the threshold of interest $c = 0.75$, we aim to target those with $\mathbb{P}(Y = 1|X) > 0.75$, i.e., target all the green segments of the sine curve.

In this example, we impose the restriction that the policymaker can only split the population *once* based on the value of X .² CART splits at $s = 0.5$, denoted as s^{CART} in Figure 1a. The left node has $\mathbb{P}(Y = 1|X > 0.5) = 0.5 + \frac{1}{\pi} > 0.75$,

served binary outcome) whose threshold is 0.5.

²This example is purely illustrative for our theoretical results in the later sections. We explain why this one-node fixed-feature

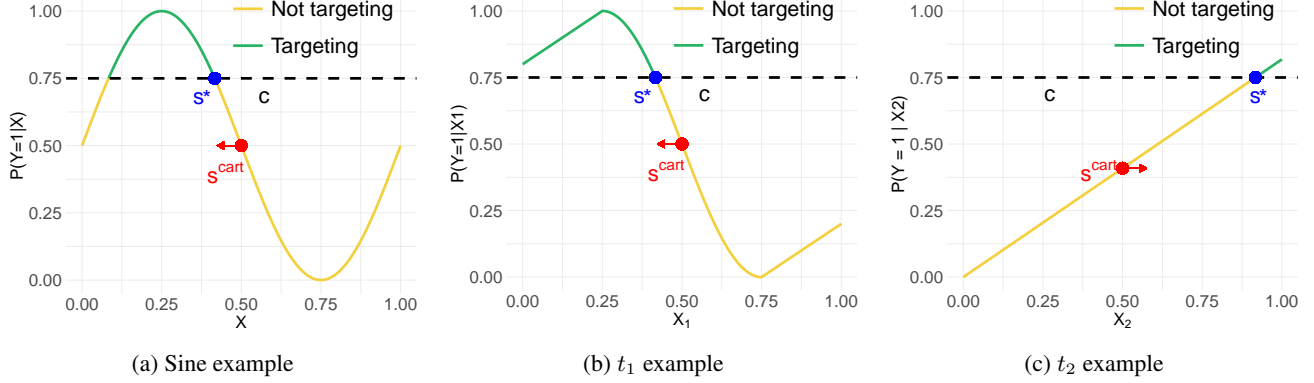


Figure 1. Three illustrative examples of η . The black dashed line indicates threshold c . The green component of η is above c (hence, should be targeted), and the yellow component of η is below c (hence, should not be targeted). s^{cart} is the split generated by CART, s^* is as defined in Theorem 2.4 in Section 3. In all three examples, s^* is a better split than s^{cart} for classifying whether η is above or below c .

whereas the right node has $\mathbb{P}(Y = 1|X \leq 0.5) = 0.5 - \frac{1}{\pi} \leq 0.75$. Consequently, we target the subpopulation by $X \leq 0.5$, i.e., left node.

To demonstrate why s^{CART} is suboptimal for the LPC problem, consider a better split at $s^* = \frac{5}{12}$. The left node still has $\mathbb{P}(Y = 1|X \leq \frac{5}{12}) \approx 0.856 > 0.75$, right node has $\mathbb{P}(Y = 1|X > \frac{5}{12}) \approx 0.246 < 0.75$. Only the left node ($X \leq \frac{5}{12}$) is targeted. This reduces misclassification risk as we exclude the group with $\frac{5}{12} < X < 0.5$ whose $\eta(X) < 0.75$ from being in the targeted node (left node). Such split location ‘‘correction’’ enhances targeting accuracy for LPC, allowing policymakers to concentrate resources on the intended groups more effectively.

This paper modifies CART’s impurity function to reflect such ‘‘correction’’: we achieve this by adding a penalty term that pushes the node means, i.e. $\mathbb{P}(Y = 1|X \leq s)$ and $\mathbb{P}(Y = 1|X > s)$, away from the threshold. We further propose to maximize a weighted sum of the distances between node means and the threshold c to identify the unique best split, assuming the existence of such a split. In addition, we show that the latter modification also reduces the misclassification risk of KD-CART, generalizing this paper’s applicability to a larger class of tree-based methods used in policymaking.³

2. One-split, one-feature LPC

We first restrict the theoretical discussion of this paper to the following one-split, one-feature (OSF) LPC problem and explain why our contribution has real-life policy significance to the multiple-node, multiple-feature setup in Section 5.

setup is relevant to policymaking scenarios where many nodes and many features are involved in Section 5.

³For example, Che et al. (2015) applies KD-CART to two binary classification problems in a healthcare intervention setup.

Let $\mathcal{X} = [0, 1]$ and $\mathcal{Y} = \{0, 1\}$ be the univariate feature space and label space, respectively. Let $f : \mathcal{X} \rightarrow \mathbb{R}^+$ be a probability density function that is continuous on \mathcal{X} , F be its corresponding cumulative distribution function, and $\eta(x) := \mathbb{P}(Y = 1|X = x)$ is continuous. Consider a dataset comprising n i.i.d. samples, (X_i, Y_i) , $i = 1, \dots, n$, where $X_i \sim f$ and $Y_i \sim \text{Bernoulli}(\eta(X_i))$.

A policymaker is allowed to split the feature space one time (i.e. one-split) using the univariate feature X (i.e. fixed feature). As illustrated by the examples in the introduction, policymakers often target those subpopulations whose $\eta(X) > c$. The misclassification risk in the OSF LPC is defined as

$$R(s) = \int_0^s \mathbb{1}\{\eta(x) > c\} \mathbb{1}\{\mu_L(s) \leq c\} + \int_0^s \mathbb{1}\{\eta(x) \leq c\} \mathbb{1}\{\mu_L(s) > c\} dF(x) + \int_s^1 \mathbb{1}\{\eta(x) > c\} \mathbb{1}\{\mu_R(s) \leq c\} + \int_s^1 \mathbb{1}\{\eta(x) \leq c\} \mathbb{1}\{\mu_R(s) > c\} dF(x), \quad (1)$$

where

$$\mu_L(s) = \int_0^s \eta(x) dF(x) / F_X(s), \quad (2)$$

$$\mu_R(s) = \int_s^1 \eta(x) dF(x) / (1 - F_X(s)). \quad (3)$$

In an LPC setup, we are particularly interested in the binary classification problem with respect to the latent probability $\eta(X)$. The policy implication is that policymakers would like to target subpopulations whose probability of a bad event Y is higher than a certain threshold c .

2.1. CART does not optimize $R(s)$

Consider using CART in the OSF LPC set up. The most common criterion function optimized by CART to determine

the split s^{CART} is the weighted sum of variances of the two child nodes, i.e.,

$$s^{CART} = \arg \min_{s \in (0,1)} \mathcal{G}^{CART}(s), \quad (4)$$

where

$$\mathcal{G}^{CART}(s) = F_X(s) \text{Var}(Y|X \leq s) + (1 - F_X(s)) \text{Var}(Y|X > s). \quad (5)$$

In our case, since the outcome variable is binary, the variance of each node has a closed-form expression:

$$\text{Var}(Y|X \leq s) = \mu_L(s) - \mu_L^2(s) \quad (6)$$

$$\text{Var}(Y|X > s) = \mu_R(s) - \mu_R^2(s) \quad (7)$$

We first state a property of the CART splitting rule in Lemma 2.1. This is useful for establishing the rest of the theoretical results.

Lemma 2.1. $2\eta(s^{CART}) - \mu_L(s^{CART}) - \mu_R(s^{CART}) = 0$ and $\mu_L(s^{CART}) \neq \mu_R(s^{CART})$,

Proofs for all lemmas and theorems are presented in Appendix B. Next, we formalize that CART does not minimize $R(s)$.

Definition 2.2. If $\exists \{s, s'\} \in [0, 1]^2$ such that $\forall x \in [0, 1]$,

$$\begin{aligned} \mu_{t(x)}(s) > c &\implies \mu_{t(x)}(s') > c \quad \text{when } \eta(x) > c, \\ \mu_{t(x)}(s) \leq c &\implies \mu_{t(x)}(s') \leq c \quad \text{when } \eta(x) \leq c, \end{aligned}$$

where

$$\mu_{t(x)}(s) = \begin{cases} \mu_L(s) & \text{if } x \leq s, \\ \mu_R(s) & \text{if } x > s, \end{cases} \quad (8)$$

and there exists a set \mathcal{A} with a nonzero measure such that, $\forall x \in \mathcal{A}$, either one (or both) of the following conditions is true

$$\begin{aligned} \mu_{t(x)}(s) \leq c, \mu_{t(x)}(s') > c &\quad \text{when } \eta(x) > c, \\ \mu_{t(x)}(s) > c, \mu_{t(x)}(s') \leq c &\quad \text{when } \eta(x) \leq c. \end{aligned}$$

Then we say that splitting rule s' **strictly dominates** splitting rule s .

Lemma 2.3. If splitting rule s' strictly dominates s , then $R(s') < R(s)$.

Next, we show that if c falls between the two node means, μ_L and μ_R , then there exist some splitting rules that strictly dominate s^{CART} and hence, have lower risk than the CART splitting rule.

Theorem 2.4. Suppose $c \in [c_{min}, c_{max}]$ where $c_{min} = \min(\mu_L(s^{CART}), \mu_R(s^{CART}))$ and $c_{max} =$

$\max(\mu_L(s^{CART}), \mu_R(s^{CART}))$ and $\eta(s^{CART}) \neq c$. There exists

$$s^* = \begin{cases} \arg \min_{s \in [0, s^{CART}], \eta(s)=c} (s^{CART} - s) & \text{if} \\ (\eta(s^{CART}) - c)(\mu_R(s^{CART}) - \mu_L(s^{CART})) > 0, \\ \arg \min_{s \in (s^{CART}, 1], \eta(s)=c} (s - s^{CART}) & \text{if} \\ (\eta(s^{CART}) - c)(\mu_R(s^{CART}) - \mu_L(s^{CART})) < 0. \end{cases}$$

Splitting node t at any $s \in [s^*, s^{CART}]$ if $s^* < s^{CART}$ **strictly dominates** $(s^{CART}, s^*]$ if $s^* > s^{CART}$ s^{CART} , and the risk difference $R(s^{CART}) - R(s)$ is continuously monotone increasing with respect to $|s - s^{CART}|$.

Lemma 2.1 and the assumption that $c \in [c_{min}, c_{max}]$ jointly guarantee the existence of s^* . When s ranges from s^{CART} to s^* , the orders of μ_L , μ_R , and c are preserved. Thus, moving from s^{CART} to s^* classifies more points into the correct categories following the intuition illustrated by Figure 1a.

2.2. KD-CART does not optimize $R(s)$

Knowledge distillation (KD) refers to a two-step learning algorithm. The first step trains a teacher model with a higher learning capacity. In the OSF LPC setup, a teacher model learns $\eta(x)$, $x \in [0, 1]$, denote the teacher model's prediction as $\hat{\eta}(x)$. The second step trains a student model which takes $\hat{\eta}(x)$ as the response variable. The goal of the student model is to output a simple/interpretable representation of the teacher model's knowledge. In the OSF LPC setup, the student model is a CART that takes in $\hat{\eta}(x)$ as the response and learns to partition the population based on $\hat{\eta}(x)$.

To explore the theoretical property of KD-CART, we treat it as a CART that takes true $\eta(x)$ as input and splits the population based on $\eta(x)$. KD-CART uses criterion function $\mathcal{G}^{KD} := F_X(s) \text{Var}(\eta(X)|X \leq s) + (1 - F_X(s)) \text{Var}(\eta(X)|X > s)$.

Lemma 2.5. Define $s^{KD} := \arg \min_{s \in (0,1)} \mathcal{G}^{KD}(s)$. $2\eta(s^{KD}) - \mu_L(s^{KD}) - \mu_R(s^{KD}) = 0$ and $\mu_L(s^{KD}) \neq \mu_R(s^{KD})$.

Theorem 2.4 also applies to s^{KD} , as proof of Theorem 2.4 only requires that $\eta(s^{CART})$ is strictly between μ_L and μ_R , Lemma 2.5 shows that $\eta(s^{KD})$ satisfies this condition.

3. Modifying Final Splits

The suboptimality of CART and KD-CART for solving OSF LPC problem motivates our proposed methods: Penalized Final Split (PFS) and Maximizing Distance Final Split (MDFS). PFS improves the split by adding a penalty

function of $|\mu_L(s) - c|$ and $|\mu_R(s) - c|$ on top of \mathcal{G} , shifting s^{CART} towards s^* . MDFS, on the other hand, maximizes a weighted sum of $|\mu_L(s) - c|$ and $|\mu_R(s) - c|$. Given there exists a unique intersection between $\eta(x)$ and c , MDFS is able to point-identify s^* such that $\eta(s^*) = c$.

Since our theoretical results guarantee a lower risk than CART's splitting rule based on one given node and feature, we advocate using our methods at the final splits with features identified by CART. Restricting modifications to the last splits may appear trivial at first, however, note that as the tree grows deeper, the number of final splits increases exponentially, leading to non-trivial modifications to the policy designs. We substantiate this claim with empirical applications in Section 7.2.

3.1. PFS

Given our specific interest in classification based on whether $\eta(X) < c$, we propose modifying the classic impurity function \mathcal{G}^{CART} used to determining the split point s . Intuitively, if μ_L is close to c and it is slightly higher than c , by the continuity assumption on η , it's highly likely that there is a considerable amount of subpopulation from the left node with $\eta(x) < c$ (see Figure 1a for an example). Following this intuition, we consider adding a penalty to \mathcal{G}^{CART} that discourages μ_L and μ_R from staying too close to c . Let

$$\mathcal{G}^{PFS}(s, c) = \mathcal{G}^{CART} + \lambda \left[F_X(s)W(|\mu_L - c|) + (1 - F_X(s))W(|\mu_R - c|) \right], \quad (9)$$

where $W : \mathbb{R}^+ \cup 0 \rightarrow \mathbb{R}^+ \cup 0$ is a decreasing function that penalizes small distances between the node means and c , and $\lambda \geq 0$ controls the weight of W .

Theorem 3.1. *Suppose $W : \mathbb{R}^+ \rightarrow \mathbb{R}^+$ is convex, monotone decreasing, and upper bounded in second derivative. If s^{CART} is the unique minimizer for \mathcal{G} , then there exists a $\Lambda > 0$ and $\eta(s^{CART}) \neq c$, such that for all $\lambda \in (0, \Lambda)$, $s^{PFS} := \arg \min_{s \in [0, 1]} \mathcal{G}^{PFS}(s, c)$ strictly dominates s^{CART} .*

We use Figure 1a to illustrate the intuition behind Theorem 3.1. In this example, $\mu_L(s^{CART}) > \mu_R(s^{CART})$. Given $\mu_L(s^{CART}) + \mu_R(s^{CART}) = 2\eta(s^{CART})$ (Lemma 2.1) and $c = 0.75 > 0.5 = \eta(s^{CART})$, μ_L is closer to c than μ_R to c . When s moves slightly to the left of s^{CART} , μ_L increases and is pushed away from the threshold. Although μ_R is pulled closer to the threshold, the monotonicity and convexity of the weight function W guarantee that the decrease in the penalty from pushing $\mu_L(s)$ away from c is larger in magnitude than the increase in penalty from pulling $\mu_R(s)$ closer to c . Hence, the penalty term incentivizes moving the split from s^{CART} towards s^* .

Corollary 3.2. *Suppose λ is chosen according to Theorem*

3.1, then $R(s^{PFS}) < R(s^{CART})$.

3.2. MDFS

PFS guarantees risk reduction with a properly chosen λ . However, it does not identify s^* . In this section, we propose a way to point-identify s^* when s^* is the unique intersection between $\eta(x)$ and c . We will explain why point-identification of s^* is of policy significance in Section 5.

Assumption 3.3. *$X \sim Unif[0, 1]$, there exists a unique s^* such that $\eta(s^*) = c$, and $\eta(X)$ is strictly monotonic and differentiable on $[s^* - \epsilon, s^* + \epsilon]$ for some $\epsilon > 0$, a neighborhood of s^* .*

We argue that Assumption 3.3 is not too restrictive because (i) the set of quantile statistics for any continuous feature follows a uniform distribution (ii) the unique intersect condition is met when $\eta(X)$ is monotonic. Monotonicity of $\eta(X)$ is a reasonable assumption that is easy to check for many empirical applications.

Theorem 3.4. *Under Assumption 3.3, $\arg \max_s \mathcal{G}^*(s, c)$ identifies s^* , where $\mathcal{G}^*(s, c) = s|\mu_L - c| + (1-s)|\mu_R - c|$.*

The proof of Theorem 3.4 can be largely decomposed into two steps: first, we show that there exists an interval containing s^* in which first-order condition guarantees that s^* is the local minima; second, we show that for all s outside of the said interval, $\mathcal{G}^*(s, c) < \mathcal{G}^*(s^*, c)$.

The unique intersect condition in Assumption 3.3 is attained when $\eta(X)$ is monotonic. Hence, Theorem 3.4 yields the following Corollary.

Corollary 3.5. *If $X \sim Unif[0, 1]$, and $\eta(X)$ is monotonic $\forall X \in [0, 1]$ and is strictly monotonic and differentiable in a neighborhood of s^* , then $\arg \max_s \mathcal{G}^*(s, c)$ identifies s^* .*

4. Large sample property of MDFS estimator

In finite sample regime, we estimate LPC policy s^* using $\{(X_i, Y_i)\}_{i=1}^n$ by maximizing the sample analogue of $\mathcal{G}^*(s, c)$. For any $\epsilon > 0$, we have $s^* \in (\epsilon, 1 - \epsilon)$ following Assumption 3.3. The MDFS final split estimator \hat{s} is defined as

$$\hat{s} = \arg \max_{s \in (\epsilon, 1 - \epsilon)} \hat{\mathcal{G}}^*(s, c), \quad (10)$$

where

$$\hat{\mathcal{G}}^*(s, c) = s \left| \frac{\sum_{i=1}^n Y_i \mathbb{1}\{X_i \leq s\}}{\sum_{i=1}^n \mathbb{1}\{X_i \leq s\}} - c \right| + (1-s) \left| \frac{\sum_{i=1}^n Y_i \mathbb{1}\{X_i > s\}}{\sum_{i=1}^n \mathbb{1}\{X_i > s\}} - c \right| \quad (11)$$

is the estimator of $\mathcal{G}^*(s, c)$.

Theorem 4.1. Under Assumption 3.3, $\hat{s} \xrightarrow{P} s^*$ as $n \rightarrow \infty$.

Theorem 4.1 is the key result for establishing convergence property of risks. On the population level, $R^* := \inf_{s \in [0,1]} R(s) = 0$ by Assumption 3.3, since s^* correctly classifies whether $\eta(x)$ is above $c \forall x \in [0, 1]$. We show that the difference between the risk associated with MDFS estimator converges in probability to $R^* = 0$.

Definition 4.2. A splitting rule \hat{s} is said to be **Risk-consistent** if $R(\hat{s}) \xrightarrow{P} 0$ as $n \rightarrow \infty$.

Corollary 4.3. \hat{s} is Risk-consistent.

Proof. $R(s)$ is continuous at s^* . Given Theorem 4.1, $R(\hat{s}) \xrightarrow{P} R(s^*) = 0$ by Continuous Mapping Theorem. \square

5. Policy Significance of LPC

In Section 2, 3 and 4, we show that baseline methods, which are the predominant practice in empirical research, do not optimize LPC, while MDFS does. It is natural for one to ask why we should care about LPC in the first place. To answer this question, here we demonstrate two advantages of LPC policies: (i) targeting more vulnerable subpopulations than CART by using the same amount of resources and (ii) uncovering subgroups with a higher-than-threshold probability of event $Y = 1$ that CART ignores.

Imagine there are two nodes $\{t_1, t_2\}$ with the same mass of population and corresponding features $X_1, X_2 \sim \text{Unif}(0, 1)$. We depict $\eta_1(X_1)$ for node t_1 in Figure 1b and $\eta_2(X_2)$ for node t_2 in Figure 1c. The analytical forms of $\eta_1(X_1)$ and $\eta_2(X_2)$ are provided in Appendix B. Here we compare the targeted population using LPC policy versus CART policy.⁴

Splitting nodes t_1 and t_2 individually at s^{CART} versus s^* results in different target subpopulations:

- s^{CART} : Target $\{X_1 < \frac{1}{2} | t_1\}$.
- s^* : Target $\{X_1 < \frac{5}{12} | t_1\}$ and $\{\frac{11}{12} < X_2 < 1 | t_2\}$.

Assuming that both t_1 and t_2 contain the same amount of population, the two sets of policies target the same proportion of the population, but $\eta_1(x) < 0.75$ for $x \in \{\frac{5}{12} < X_1 < \frac{1}{2}\}$, which is targeted by s^{CART} , whereas $\eta_2(x) > 0.75$ for $x \in \{\frac{11}{12} < X_2 < 1\}$, which is targeted by s^* . Therefore, policies based on LPC, i.e., s^* policy, target a **more vulnerable** subpopulation than CART/KD-CART policy. This idea corresponds to our diabetes empirical study in Section 7.2.

⁴In these two examples, CART and KD-CART generate identical policies because $\eta(x)$ is reflectional symmetric around $x = 0.5$.

Admittedly, the fact that LPC and CART policies target the same proportion of the population in the previous example is by construction. It is also possible that the proportion of the population targeted by the LPC policy is bigger than that by CART or KD-CART. In this scenario, comparing the effectiveness of the two sets of policies is not straightforward. Nonetheless, LPC still has policy significance. It discovers new latent groups with a higher probability of a bad event than the threshold, e.g. $\eta_2(x) > 0.75$ for $\frac{11}{12} < x < 1$.

We make two remarks of Theorem 2.4 to formalize the two advantages that LPC policy offers.⁵ Assuming a homogeneous targeting cost per unit of population, the targeting cost of a policy is the percentage of the subpopulation targeted. Denote all M final splitting nodes as $\{t_1, t_2, \dots, t_M\}$ and $\mathcal{M} = \{1, 2, \dots, M\}$. For node m , we denote the feature selected by CART as $X_{(m)}$ and the CDF of $X_{(m)}$ as F_m and let $\eta_m(x) = P(Y = 1 | X_{(m)} = x)$. The cost of CART and LPC policies are

$$C^{CART} = \sum_{m \in \mathcal{M}} \int_0^1 \mathbb{1}\{\mu_{t(x)}(s_m^{CART}) > c\} dF_m(x) \quad (12)$$

$$C^* = \sum_{m \in \mathcal{M}} \int_0^1 \mathbb{1}\{\mu_{t(x)}(s_m^*) > c\} dF_m(x) \quad (13)$$

Assume that for some $m \in \mathcal{M}$, $s_m^{CART} \neq s_m^*$.

Remark 5.1. If $C^{CART} = C^*$, then LPC policy targets strictly more vulnerable (greater $\eta_m(X_{(m)})$) subpopulation than CART using the same targeting resources.

Remark 5.2. If $C^{CART} < C^*$, then LPC policy uncovers latent subgroups in some node m with selected feature $X_{(m)} = x$ whose $\eta_m(x) > c$ that CART ignores.

6. Related literature

Cost-sensitive binary classification: The LPC policy can be related to the optimal solution of a cost-sensitive binary classification problem, further highlighting the policy significance of the LPC problem. Nan et al. (2012); Menon et al. (2013); Koyejo et al. (2014) show that the optimal classifier of a cost-sensitive binary classification problem is determined by whether the latent probability is above some performance-metric-dependent threshold. Hence, we modify weighted ERM, a popular approach in the literature to our setup. However, whether the theoretical results in the cost-sensitive classification literature carry over to our setup is unclear. For example, Nan et al. (2012) shows risk consistency with uniform convergence of the empirical risk. In our setup, $\{\mu_L(s), \mu_R(s)\}$ appear inside the indicator functions, and uniform convergence of empirical risk is not guaranteed

⁵The two Remarks also hold if we replace CART with KD-CART.

Modifying Final Splits of Classification Tree for Fine-tuning Subpopulation Target in Policy Making

DGP	c	CART	PFS	MDFS	wEFS	RF-CART	RF-MDFS
Ball	0.8	9.6 (1.9)	9.2 (1.7)	9.2 (1.4)	9.2 (1.4)	8.8 (1.8)	8.6 (1.4)
	0.7	14.5 (2.4)	14.2 (2.2)	13.7 (2.3)	13.7 (2.3)	13.2 (2.1)	12.6 (1.8)
	0.6	14.9 (1.7)	14.5 (1.9)	14.1 (1.4)	14.1 (1.5)	13.9 (1.9)	13.2 (1.5)
Friedman #1	0.8	6.8 (1.3)	6.7 (1.3)	6.7 (1.4)	6.7 (1.4)	6.0 (1.0)	6.3 (1.0)
	0.7	12.7 (1.6)	12.6 (1.5)	12.5 (1.3)	12.5 (1.3)	11.8 (1.3)	11.7 (1.1)
	0.6	18.5 (1.7)	18.4 (1.6)	18.2 (1.5)	18.2 (1.5)	18.1 (1.5)	18.0 (1.3)
Friedman #2	0.8	8.8 (2.2)	8.0 (1.6)	7.5 (1.5)	7.5 (1.5)	8.4 (1.7)	7.3 (1.3)
	0.7	8.2 (1.7)	7.9 (1.6)	7.7 (1.5)	7.7 (1.5)	7.9 (1.9)	7.4 (1.6)
	0.6	6.9 (1.5)	6.7 (1.5)	6.4 (1.4)	6.4 (1.5)	6.7 (1.9)	6.2 (1.3)
Friedman #3	0.8	2.0 (0.5)	2.0 (0.5)	2.0 (0.5)	2.0 (0.5)	1.9 (0.5)	1.9 (0.5)
	0.7	2.5 (0.5)	2.5 (0.6)	2.4 (0.5)	2.4 (0.5)	2.4 (0.5)	2.4 (0.5)
	0.6	3.2 (0.7)	3.3 (0.7)	3.0 (0.5)	3.0 (0.5)	3.1 (0.5)	3.0 (0.5)
Poly #1	0.8	7.3 (1.4)	7.2 (1.3)	7.3 (1.2)	7.3 (1.2)	7.2 (1.3)	7.0 (1.1)
	0.7	11.0 (2.4)	10.4 (2.1)	10.1 (1.7)	10.1 (1.7)	9.9 (1.9)	9.4 (1.5)
	0.6	12.9 (2.0)	12.6 (2.8)	12.2 (2.7)	12.2 (2.6)	12.1 (1.8)	11.9 (2.6)
Poly #2	0.8	10.1 (2.5)	10.0 (2.2)	9.9 (2.1)	9.9 (2.2)	9.6 (2.1)	9.4 (2.0)
	0.7	9.8 (2.2)	9.5 (1.9)	9.4 (1.8)	9.5 (1.8)	9.6 (1.9)	9.6 (1.6)
	0.6	8.7 (1.9)	8.5 (1.6)	8.0 (1.5)	8.0 (1.5)	8.1 (1.6)	7.6 (1.3)
Ring	0.8	18.9 (2.3)	19.0 (2.5)	18.6 (2.7)	18.5 (2.6)	17.4 (2.3)	17.5 (2.4)
	0.7	15.6 (2.0)	15.7 (2.3)	15.5 (2.3)	15.5 (2.3)	14.3 (1.8)	14.3 (1.7)
	0.6	13.2 (1.7)	13.1 (1.5)	12.7 (1.4)	12.7 (1.4)	12.1 (1.4)	11.8 (1.5)
Collinear	0.8	6.8 (1.7)	6.7 (1.6)	6.3 (1.5)	6.3 (1.5)	6.3 (1.4)	5.9 (1.3)
	0.7	7.7 (1.4)	7.7 (1.4)	7.3 (1.2)	7.3 (1.2)	7.2 (1.7)	7.0 (1.0)
	0.6	8.5 (1.4)	8.2 (1.2)	7.9 (1.2)	7.9 (1.2)	8.4 (1.3)	7.8 (1.2)

Table 1. Comparison of misclassification error among CART, PFS, MDFS, and wEFS using raw data input, and CART, and MDFS using random forest as KD tool. Each entry presents the average and standard deviation (in parentheses) of the misclassification error over 50 experiments.

even with a large sample. Another example is that [Koyejo et al. \(2014\)](#) proves risk-consistency of weighted ERM assuming that the policymakers search through all real-valued functions. In our setup, policymakers only search among threshold-type policies.

Knowledge distillation: [Liu et al. \(2018\)](#); [Dao et al. \(2021\)](#) use CART as the student model in knowledge distillation. We show that some of the theoretical results we develop for CART apply to their work (termed KD-CART in our paper).

7. Experiments

In this section, we conduct comprehensive numerical experiments to compare the performance of our proposed algorithms and the classic CART under both regular and KD frameworks. Under regular framework, we compare the classic CART with PFS and MDFS. Under KD framework, we compare RF-CART with RF-MDFS. We replace KD with RF because the teacher model is a **R**andom **F**orest. In

addition, we adapt Proposition 6 from [Koyejo et al. \(2014\)](#) to the final split and refer to the adapted method as wEFS (weighted Empirical Final Split).

7.1. Synthetic Data

Settings: We simulate synthetic datasets using 8 different data generation processes (DGP), e.g., the Friedman synthetic datasets ([Friedman, 1991](#); [Breiman, 1996](#)). These setups are designed to capture various aspects of real-world data complexities and challenges commonly encountered when using tree-based method, such as nonlinear relationships, feature interactions, collinearity, and noises (Table 1, Column 1). Detailed descriptions of the DGP are provided in Appendix C.1. For each DGP, we consider a threshold of interest $c \in \{0.6, 0.7, 0.8\}$, resulting in 24 unique tasks.

We set two stopping rules for growing the tree: (i) a max depth of $m \in \{4, 5, 6, 7\}$, (ii) a minimal leaf node size of ρn , where $\rho \in \{1\%, 2\%, 3\%\}$ and n is the sample size. We set $n = 5000$. The fitting procedures stop once either of the

rules is met. These give us 12 configurations for each tasks. For each of the $24 \times 12 = 288$ settings, we do 50 replicates of experiments.

Evaluation metrics: We use the misclassification rate (MR) and the standard deviation of it to evaluate the performance and robustness of different approaches. We abuse the notation of η by defining $\eta(\mathbf{X}_i) := \mathbb{P}(Y_i = 1|\mathbf{X}_i)$ where \mathbf{X}_i is the *multivariate* feature vector which includes *all* features in the simulation.

$$\text{MR} = \frac{1}{n} \sum_{i=1}^n \mathbb{1}\{(\widehat{T}(\mathbf{X}_i) - c)(\eta(\mathbf{X}_i) - c) < 0\}, \quad (14)$$

where $\widehat{T}(\mathbf{X}_i)$ is the tree-estimate of $\eta(\mathbf{X}_i)$. Although there is a gap between this evaluation metric (using $\eta(\mathbf{X}_i)$) and our theories (using $\eta(X_i)$), we justify the use of MR in two ways. First, obtaining $\eta(X)$ for all final splits involve iterative integration of $\eta(\mathbf{X})$. In our simulation setups, $\eta(\mathbf{X})$ does not have closed-forms for their integrals. Second, MR is still of interest to policymakers. A policymaker cares about classifying individual i based on their probability of an event $Y = 1$ conditional on *all* their features.

Model fitting procedures: As we mentioned in Section 3, our methods and their counterparts only differ in the splits at the final level (final splits). We first implement CART until the final split is reached based on the stopping rules. Once the final split is identified, we select the splitting feature using CART, then implement PFS, MDFS, and wEFS with the splitting feature. MDFS and PFS decide the split by optimizing \mathcal{G}^* and \mathcal{G}^{PFS} , respectively, while wEFS selects the split by identifying s such that the minimum weighted empirical risk is obtained (see Algorithm 3 in Appendix C.2 for the computation detail of weighed empirical risk).

For W in \mathcal{G}^{PFS} from (9), we choose $W(d) = 1 - d$. This choice of W satisfies conditions specified in Theorem 3.1. We also experiment with alternative choices, such as $W(d) = (1 - d)^2$ and $W(d) = \exp(-d)$, but observed similar performance across these choices. Based on Theorem 3.1, we set $\lambda = 0.1$, a sufficiently small value that presumably satisfies the conditions of the theorem while maintaining practical effectiveness.

Results: Out of 288 simulation settings, PFS, MDFS, and wEFS outperform CART in terms of MR 78.13%, 87.15%, 88.19% of the time, respectively. In Table 1, we only present the lowest MR among all 12 configurations (max depth and minimal leaf node size combinations) for all 24 tasks (DGP and c combinations). In Table 1, PFS, MDFS, and wEFS outperform CART 83.33%, 100%, and 100% of the time, respectively.

Our methods have a clear advantage over classic CART. However, the selection of λ and uniqueness of intersection between η and c can hardly be validated in reality. The

theoretical guarantee of PFS, MDFS, and wEFS under more general conditions remains as an interesting future research direction.

Under KD framework, RF-MDFS beats RF-CART 73.6% of the time out of the 288 simulation settings, 83.3% of the time when only selecting the best configuration in each task. Due to the page limit, we present only part of the simulation results in Table 1. The complete simulation results are provided in the supplemental files.

7.2. Real-world Datasets

We implement CART, MDFS, RF-CART, and RF-MDFS with the Pima Indians Diabetes (Smith et al., 1988), to demonstrate the policy significance of our proposed methods.⁶ The empirical findings align with Remark 5.1 and 5.2. The Pima Indians Diabetes dataset measures health factors among Pima Indian women with the response variable being a binary indicator of diabetes status: 34.9% of the sample is diabetic. It contains 768 observations and 8 features: number of pregnancies, glucose level, blood pressure, skin thickness, insulin level, BMI, family diabetes history index, and age. We use these eight features to search for subpopulations whose probability of having diabetes is above 60% with depth of trees fixed at $m = 3$.

7.2.1. CART vs MDFS

As shown in Figure 2, CART and MDFS commonly target those with $Glucose > 129.5$ and $BMI > 29.95$, which consists of 188 observations. The two methods' targeting policies differ in two ways:

- CART additionally targets $127.5 < Glucose \leq 129.5$ and $BMI > 29.95$. This subgroup consists of 19 observations.
- MDFS additionally targets $Glucose > 166.5$ and $BMI \leq 29.95$. This subgroup consists of 12 observations.

The difference between the sizes of these two subgroups is 7, which is small relative to 188, i.e., the size of the subgroup commonly targeted by both policies. Assuming that the sample is representative of the population of all Pima Indian women, then the two sets of policies will incur a similar amount of targeting resources. The additional group targeted by CART has a 57.9% probability of having diabetes, whereas the additional group targeted by MDFS has a 66.7% probability of having diabetes. MDFS targets a subpopulation that is more prone to diabetes. This corresponds to Remark 5.1.

⁶We supplement an additional forest fire empirical study in Appendix D to showcase the wide applicability of our paper.

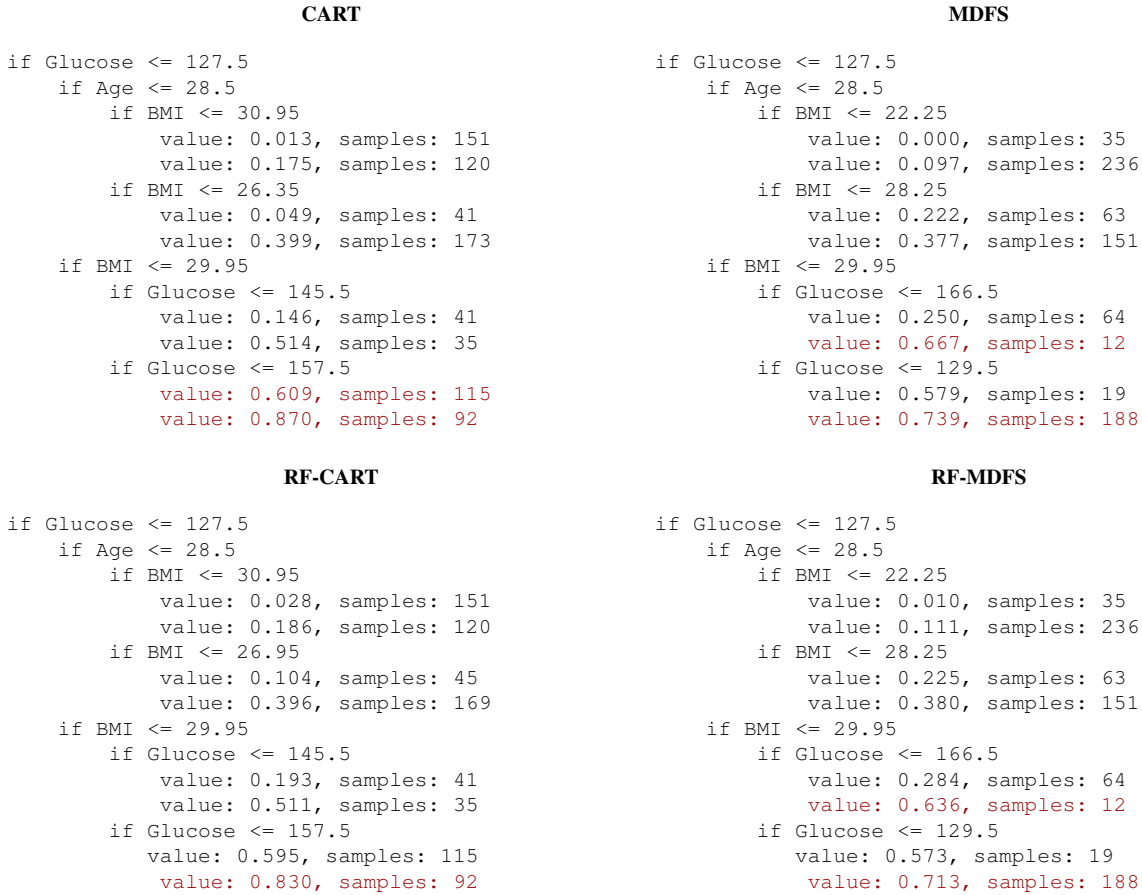


Figure 2. The targeting policies generated by CART, MDFS, RF-CART, RF-MDFS. The red groups are the targeted subpopulations predicted to a higher than 60% probability of being diabetic.

7.2.2. RF-CART vs RF-MDFS

We first use *RandomForestClassifier* from *sklearn* (Pedregosa et al., 2011) to train a random forest with the entire sample. All user-defined parameters of the random forest follow the default settings. Then, we grow an RF-CART and an RF-MDFS tree with the predicted probability output by the random forest as the response variable.

As shown in Figure 2, both RF-CART and RF-MDFS commonly target $Glucose > 157.5$ and $BMI > 29.95$, a subgroup consisting of 88 observations. RF-MDFS additionally targets two subgroups:

- $Glucose > 166.5$ and $BMI \leq 29.95$ consisted of 12 observations and
- $129.5 < Glucose \leq 157.5$ and $BMI > 29.95$ consisted of 96 observations.

RF-MDFS targets a much greater number of observations than RF-CART. If the sample is representative of the population, then RF-MDFS would use much more targeting

resources than RF-CART. Nevertheless, RF-MDFS is useful in uncovering groups with higher than 60% probability of having diabetes that RF-CART is unable to find. For example, the first group that RF-MDFS additionally targets has a 63.6% probability of having diabetes. This aligns with Remark 5.2.

8. Conclusion

Our paper points out that the classic CART does not directly minimize LPC misclassification risk in each split. Based on different assumptions, we propose two alternative methods PFS and MDFS, both of which reduces LPC misclassification risk. The applicability of the theoretical results also extend to KD-CART. Our proposed methods predominantly outperform their counterparts in our simulation and provide more policy insights in empirical applications.

There are multiple interesting future work directions. First, as mentioned earlier, the theoretical guarantee of risk reduction for PFS and MDFS can be further investigated under more general conditions. Second, in the current version

of this paper, KD-MDFS extends the applicability of our theories to $\eta(x)$ being the response variable which takes on continuous value, extending it further to more general continuous outcome problems can be interesting. Third, the idea of latent probability classification can be adapted to other cost-sensitive machine learning algorithms (Babii et al., 2020) and provide more insights for policy making.

Impact Statement

This paper presents work whose goal is to advance the field of Machine Learning. There are many potential societal consequences of our work, none which we feel must be specifically highlighted here.

References

- Alexiou, S., Dritsas, E., Kocsis, O., Moustakas, K., and Fakotakis, N. An approach for personalized continuous glucose prediction with regression trees. In *2021 6th South-East Europe Design Automation, Computer Engineering, Computer Networks and Social Media Conference (SEEDA-CECNSM)*, pp. 1–6. IEEE, 2021.
- Ali, Ö. G., Sayın, S., Van Woensel, T., and Fransoo, J. Sku demand forecasting in the presence of promotions. *Expert Systems with Applications*, 36(10):12340–12348, 2009.
- Andini, M., Ciani, E., de Blasio, G., D’Ignazio, A., and Salvestrini, V. Targeting with machine learning: An application to a tax rebate program in italy. *Journal of Economic Behavior & Organization*, 156:86–102, 2018.
- Athey, S. and Imbens, G. Recursive partitioning for heterogeneous causal effects. *Proceedings of the National Academy of Sciences*, 113(27):7353–7360, 2016.
- Athey, S. and Wager, S. Policy learning with observational data. *Econometrica*, 89(1):133–161, 2021.
- Athey, S., Wager, S., Tibshirani, J., et al. Generalized random forests. *The Annals of Statistics*, 47(2):1148–1178, 2019.
- Babii, A., Chen, X., Ghysels, E., and Kumar, R. Binary choice with asymmetric loss in a data-rich environment: Theory and an application to racial justice. *arXiv preprint arXiv:2010.08463*, 2020.
- Biau, G. Analysis of a random forests model. *Journal of Machine Learning Research*, 13:1063–1095, 2012.
- Biau, G., Devroye, L., and Lugosi, G. Consistency of random forests and other averaging classifiers. *Journal of Machine Learning Research*, 9(9), 2008.
- Blanc, G., Lange, J., and Tan, L.-Y. Provable guarantees for decision tree induction: the agnostic setting. In *International Conference on Machine Learning*, pp. 941–949. PMLR, 2020.
- Blanc, G., Lange, J., Qiao, M., and Tan, L.-Y. Properly learning decision trees in almost polynomial time. *Journal of the ACM*, 69(6):1–19, 2022.
- Breiman, L. Bagging predictors. *Machine learning*, 24: 123–140, 1996.
- Breiman, L. Random forests. *Machine Learning*, 45(1): 5–32, 2001.
- Breiman, L. *Classification and regression trees*. Routledge, 2017.
- Brutzkus, A., Daniely, A., and Malach, E. Id3 learns juntas for smoothed product distributions. In *Conference on Learning Theory*, pp. 902–915. PMLR, 2020.
- Che, Z., Purushotham, S., Khemani, R., and Liu, Y. Distilling knowledge from deep networks with applications to healthcare domain. *arXiv preprint arXiv:1512.03542*, 2015.
- Çığışar, B. and Ünal, D. Comparison of data mining classification algorithms determining the default risk. *Scientific Programming*, 2019(1):8706505, 2019.
- Clarke, D. D., Forsyth, R., and Wright, R. Machine learning in road accident research: decision trees describing road accidents during cross-flow turns. *Ergonomics*, 41(7): 1060–1079, 1998.
- Costa, V. G. and Pedreira, C. E. Recent advances in decision trees: An updated survey. *Artificial Intelligence Review*, 56(5):4765–4800, 2023.
- Crowe, M., O’Sullivan, M., Cassetti, O., and O’Sullivan, A. Weight status and dental problems in early childhood: classification tree analysis of a national cohort. *Dentistry Journal*, 5(3):25, 2017.
- da Cruz Figueira, A., Pitombo, C. S., Larocca, A. P. C., et al. Identification of rules induced through decision tree algorithm for detection of traffic accidents with victims: A study case from brazil. *Case Studies on Transport Policy*, 5(2):200–207, 2017.
- Dao, T., Kamath, G. M., Syrgkanis, V., and Mackey, L. Knowledge distillation as semiparametric inference. *arXiv preprint arXiv:2104.09732*, 2021.
- Duan, L. and Xu, L. Classification based on multiple association rules. *ACM Transactions on Intelligent Systems and Technology (TIST)*, 2(4):35, 2011.
- Efron, B. Estimation and accuracy after model selection. *Journal of the American Statistical Association*, 109(507): 991–1007, 2014.
- Feldman, D. and Gross, S. Mortgage default: classification trees analysis. *The Journal of Real Estate Finance and Economics*, 30:369–396, 2005.
- Friedman, J. H. Multivariate adaptive regression splines. *The annals of statistics*, 19(1):1–67, 1991.

- Gao, W. and Zhou, Z.-H. Towards convergence rate analysis of random forests for classification. *Advances in neural information processing systems*, 33:9300–9311, 2020.
- Guelman, L. Gradient boosting trees for auto insurance loss cost modeling and prediction. *Expert Systems with Applications*, 39(3):3659–3667, 2012.
- Gulowaty, B. and Woźniak, M. Extracting interpretable decision tree ensemble from random forest. In *2021 International Joint Conference on Neural Networks (IJCNN)*, pp. 1–8. IEEE, 2021.
- Hannan, A. and Anmala, J. Classification and prediction of fecal coliform in stream waters using decision trees (DTs) for upper Green River watershed, Kentucky, USA. *Water*, 13(19):2790, 2021.
- Herman, J. D. and Giuliani, M. Policy tree optimization for threshold-based water resources management over multiple timescales. *Environmental Modelling & Software*, 99: 39–51, 2018.
- Hwang, S., Yeo, H. G., and Hong, J.-S. A new splitting criterion for better interpretable trees. *IEEE Access*, 8: 62762–62774, 2020.
- Kalai, A. T. and Teng, S.-H. Decision trees are pac-learnable from most product distributions: a smoothed analysis. *arXiv preprint arXiv:0812.0933*, 2008.
- Kallus, N. Recursive partitioning for personalization using observational data. In *International conference on machine learning*, pp. 1789–1798. PMLR, 2017.
- Kashani, A. T. and Mohaymany, A. S. Analysis of the traffic injury severity on two-lane, two-way rural roads based on classification tree models. *Safety Science*, 49 (10):1314–1320, 2011.
- Kitagawa, T. and Tetenov, A. Who should be treated? empirical welfare maximization methods for treatment choice. *Econometrica*, 86(2):591–616, 2018.
- Klusowski, J. M. Universal consistency of decision trees in high dimensions. *arXiv preprint arXiv:2104.13881*, 2021.
- Kotsiantis, S. B. Decision trees: a recent overview. *Artificial Intelligence Review*, 39:261–283, 2013.
- Koyejo, O. O., Natarajan, N., Ravikumar, P. K., and Dhillon, I. S. Consistent binary classification with generalized performance metrics. *Advances in neural information processing systems*, 27, 2014.
- Lakshmi, S. and Kavilla, S. D. Machine learning for credit card fraud detection system. *International Journal of Applied Engineering Research*, 13(24):16819–16824, 2018.
- Lee, M. S. A. and Floridi, L. Algorithmic fairness in mortgage lending: from absolute conditions to relational trade-offs. *Minds and Machines*, 31(1):165–191, 2021.
- Li, R.-H. and Belford, G. G. Instability of decision tree classification algorithms. In *Proceedings of the eighth ACM SIGKDD international conference on Knowledge discovery and data mining*, pp. 570–575, 2002.
- Lin, Y. and Jeon, Y. Random forests and adaptive nearest neighbors. *Journal of the American Statistical Association*, 101(474):578–590, 2006.
- Liu, X., Wang, X., and Matwin, S. Improving the interpretability of deep neural networks with knowledge distillation. In *2018 IEEE International Conference on Data Mining Workshops (ICDMW)*, pp. 905–912. IEEE, 2018.
- Madaan, M., Kumar, A., Keshri, C., Jain, R., and Nagrath, P. Loan default prediction using decision trees and random forest: A comparative study. In *IOP Conference Series: Materials Science and Engineering*, volume 1022, pp. 012042. IOP Publishing, 2021.
- Mahendran, M., Lizotte, D., and Bauer, G. R. Quantitative methods for descriptive intersectional analysis with binary health outcomes. *SSM-Population Health*, 17: 101032, 2022.
- Mann, J. J., Ellis, S. P., Waternaux, C. M., Liu, X., Oquendo, M. A., Malone, K. M., Brodsky, B. S., Haas, G. L., and Currier, D. Classification trees distinguish suicide attempters in major psychiatric disorders: a model of clinical decision making. *Journal of Clinical Psychiatry*, 69 (1):23, 2008.
- Mashat, A. F., Fouad, M. M., Philip, S. Y., and Gharib, T. F. A decision tree classification model for university admission system. *International Journal of Advanced Computer Science and Applications*, 3(10), 2012.
- Mbakop, E. and Tabord-Meehan, M. Model selection for treatment choice: Penalized welfare maximization. *Econometrica*, 89(2):825–848, 2021.
- Meinshausen, N. Quantile regression forests. *Journal of Machine Learning Research*, 7:983–999, 2006.
- Menon, A., Narasimhan, H., Agarwal, S., and Chawla, S. On the statistical consistency of algorithms for binary classification under class imbalance. In *International Conference on Machine Learning*, pp. 603–611. PMLR, 2013.
- Mentch, L. and Hooker, G. Quantifying uncertainty in random forests via confidence intervals and hypothesis tests. *The Journal of Machine Learning Research*, 17(1): 841–881, 2016.

- Nan, Y., Chai, K. M., Lee, W. S., and Chieu, H. L. Optimizing f-measure: A tale of two approaches. *arXiv preprint arXiv:1206.4625*, 2012.
- Obereigner, G., Tkachenko, P., and del Re, L. Methods for traffic data classification with regard to potential safety hazards. *IFAC-PapersOnLine*, 54(7):250–255, 2021.
- Pedregosa, F., Varoquaux, G., Gramfort, A., Michel, V., Thirion, B., Grisel, O., Blondel, M., Prettenhofer, P., Weiss, R., Dubourg, V., Vanderplas, J., Passos, A., Cournapeau, D., Brucher, M., Perrot, M., and Duchesnay, E. Scikit-learn: Machine learning in Python. *Journal of Machine Learning Research*, 12:2825–2830, 2011.
- Piwczyński, D., Sitkowska, B., Kolenda, M., Brzozowski, M., Aerts, J., and Schork, P. M. Forecasting the milk yield of cows on farms equipped with automatic milking system with the use of decision trees. *Animal Science Journal*, 91(1):e13414, 2020.
- Quinlan, J. R. *C4. 5: programs for machine learning*. Elsevier, 2014.
- Saghebian, S. M., Sattari, M. T., Mirabbasi, R., and Pal, M. Ground water quality classification by decision tree method in ardebil region, iran. *Arabian Journal of Geosciences*, 7:4767–4777, 2014.
- Sagi, O. and Rokach, L. Explainable decision forest: Transforming a decision forest into an interpretable tree. *Information Fusion*, 61:124–138, 2020.
- Sagi, O. and Rokach, L. Approximating XGBoost with an interpretable decision tree. *Information Sciences*, 572:522–542, 2021.
- Sahin, Y., Bulkan, S., and Duman, E. A cost-sensitive decision tree approach for fraud detection. *Expert Systems with Applications*, 40(15):5916–5923, 2013.
- Sarkar, M. S., Majhi, B. K., Pathak, B., Biswas, T., Mahapatra, S., Kumar, D., Bhatt, I. D., Kuniyal, J. C., and Nautiyal, S. Ensembling machine learning models to identify forest fire-susceptible zones in northeast india. *Ecological Informatics*, 81:102598, 2024.
- Save, P., Tiwarekar, P., Jain, K. N., and Mahyavanshi, N. A novel idea for credit card fraud detection using decision tree. *International Journal of Computer Applications*, 161(13), 2017.
- Scornet, E., Biau, G., and Vert, J.-P. Consistency of random forests. *The Annals of Statistics*, 43(4):1716–1741, 2015.
- Sexton, J. and Laake, P. Standard errors for bagged and random forest estimators. *Computational Statistics & Data Analysis*, 53(3):801–811, 2009.
- Shouman, M., Turner, T., and Stocker, R. Using decision tree for diagnosing heart disease patients. *AusDM*, 11:23–30, 2011.
- Smith, J. W., Everhart, J. E., Dickson, W., Knowler, W. C., and Johannes, R. S. Using the adap learning algorithm to forecast the onset of diabetes mellitus. In *Proceedings of the annual symposium on computer application in medical care*, pp. 261. American Medical Informatics Association, 1988.
- Speiser, J. L., Karvellas, C. J., Shumilak, G., Sligl, W. I., Mirzanejad, Y., Gurka, D., Kumar, A., and Kumar, A. Predicting in-hospital mortality in pneumonia-associated septic shock patients using a classification and regression tree: a nested cohort study. *Journal of intensive care*, 6:1–10, 2018.
- Takimoto, E. and Maruoka, A. Top-down decision tree learning as information based boosting. *Theoretical Computer Science*, 292(2):447–464, 2003.
- Toth, E. G., Gibbs, D., Moczygemba, J., and McLeod, A. Decision tree modeling in r software to aid clinical decision making. *Health and Technology*, 11(3):535–545, 2021.
- Van der Vaart, A. W. *Asymptotic statistics*, volume 3. Cambridge university press, 2000.
- Varian, H. R. Big data: New tricks for econometrics. *Journal of Economic Perspectives*, 28(2):3–28, 2014.
- Wager, S. and Athey, S. Estimation and inference of heterogeneous treatment effects using random forests. *Journal of the American Statistical Association*, 113(523):1228–1242, 2018.
- Wager, S. and Walther, G. Adaptive concentration of regression trees, with application to random forests. *arXiv preprint arXiv:1503.06388*, 2015.
- Waheed, T., Bonnell, R., Prasher, S. O., and Paulet, E. Measuring performance in precision agriculture: CART—A decision tree approach. *Agricultural Water Management*, 84(1-2):173–185, 2006.
- Zheng, Q.-C., Lyu, S.-H., Zhang, S.-Q., Jiang, Y., and Zhou, Z.-H. On the consistency rate of decision tree learning algorithms. In *International Conference on Artificial Intelligence and Statistics*, pp. 7824–7848. PMLR, 2023.
- Zhu, R., Zeng, D., and Kosorok, M. R. Reinforcement learning trees. *Journal of the American Statistical Association*, 110(512):1770–1784, 2015.
- Zou, L. and Khern-am nuai, W. AI and housing discrimination: the case of mortgage applications. *AI and Ethics*, 3(4):1271–1281, 2023.

A. Further literature review

A.1. Extensive use of CART for policy targeting

Traffic safety: da Cruz Figueira et al. (2017) identifies potential sites of serious accidents in Brazil using different decision tree algorithms. Policymakers may choose to take more safety precautions at dangerous traffic spots whose probability of having a fatal accident is above a threshold. Other research that uses decision trees to identify dangerous traffic situations includes Clarke et al. (1998); Kashani & Mohaymany (2011); Obereigner et al. (2021).

Fraud detection: Sahin et al. (2013); Save et al. (2017); Lakshmi & Kavilla (2018) find conditions under which credit card fraudulent usage is likely to happen. Credit card companies can inform card owners when the probability of fraudulent usage is above a pre-specified threshold.

Mortgage lending: Feldman & Gross (2005); Çığşar & Ünal (2019); Madaan et al. (2021) predict different subpopulations' mortgage (and other types of loan) default rates using a decision tree. Mortgage loan lenders can use the result to determine whether to deny a loan request. Another stream of literature on mortgage lending using decision trees focuses on racial discrimination (Varian, 2014; Lee & Floridi, 2021; Zou & Khern-am nuai, 2023). Policymakers may want to intervene in situations where with high enough probability race seems to play a role in determining whether mortgage lending is denied and the probability of denial is high.

Health intervention: Mann et al. (2008); Shouman et al. (2011); Crowe et al. (2017); Speiser et al. (2018); Toth et al. (2021); Mahendran et al. (2022) classify diabetes (or other diseases) using relevant risk factors. Such classification result leads to different health interventions. Doctors may recommend various treatments based on whether the subpopulation a patient belongs to is more likely to be classified as type I or type II diabetes.

Water management: One of the objectives of Herman & Giuliani (2018) is to manage flood control and output a threshold-based water resources management policy. The authors output a set of conditions that define the subpopulation whose probability of flooding is high enough to justify policy intervention. Many other studies also use decision trees to classify whether the water quality is satisfactory, resulting in important implications to water management policies (Waheed et al., 2006; Saghebian et al., 2014; Hannan & Anmala, 2021).

A.2. Related Literature on CART and Random Forest

On top of its empirical relevance, this paper adds to the growing theoretical literature on CART and random forests. We briefly outline several areas where our research contributes or applies.⁷

Criterion function of CART: Quinlan (2014); Breiman (2017) are two seminal works that describe CART in detail. Following the two seminal papers, most works in the field minimize some impurity measures: variance for continuous responses and Gini impurity score (or entropy) for discrete responses. There are a few attempts to modify the criterion function of CART. (1) Athey & Imbens (2016) removes the bias of CART by using two independent samples to determine data partition and estimate heterogeneous group means separately. The authors name the two samples training and estimation samples. Their criterion function depends on both, which differs from the classic criterion function that treats the entire sample as the training sample as defined by Athey & Imbens (2016). (2) Hwang et al. (2020) aims to improve the interpretability of CART. The authors define interpretability as the purity and size of the nodes: pure and big nodes lead to a more interpretable splitting rule. They modify the criterion function such that their CART tends to produce a small number of leaf nodes that are large and homogeneous, enhancing the interpretability of the splitting rule as defined in the paper. (3) Zheng et al. (2023) shows that one of the key challenges in proving the consistency of the heuristic tree learning algorithm is the potentially zero “worst-case purity gain”. The authors switch the impurity score measure of CART to an influence measure and prove that the new criterion function leads to better consistency rate results.

We contribute to the literature that modifies the criterion function of CART. The major distinction between our paper and the others is that we focus on a novel classification problem of a latent probability for a binary outcome event. This leads to a different set of theoretical results and modifications of CART. Unlike past works that focus on the bias (Athey & Imbens, 2016), interpretability (Hwang et al., 2020), or consistency (Zheng et al., 2023) properties, we define a novel risk measure and prove our method's theoretical advantage over CART regarding this new risk measure.

⁷There is a vast literature on decision trees, we do not claim this section to be all-encompassing. Readers should refer to Kotsiantis (2013); Costa & Pedreira (2023) for more comprehensive reviews.

Random Forest asymptotic: Lots of the theoretical literature on CART focuses on the asymptotic property of random forest (Biau et al., 2008; Scornet et al., 2015; Wager & Athey, 2018; Gao & Zhou, 2020; Klusowski, 2021)⁸. This literature deals with feature selection and asymptotic behavior of variants of random forests. We have a very different goal of classifying latent probability. First, we take the features selected by CART as given and hence, we are not concerned with feature selection. Second, we prove our approach leads to a smaller risk with respect to the population distribution compared to CART and does not deal with the asymptotic behavior of an estimator. Consequently, we impose a set of different assumptions.

Assumptions on f and η : We compare the assumptions made by our paper with those made by random forest learning theory literature. We require f , the distribution of covariates X , to be continuous and strictly positive over a bounded domain. It is also much weaker than the production distribution (independence across feature) assumption made by Takimoto & Maruoka (2003), Kalai & Teng (2008), Brutzkus et al. (2020) and Zheng et al. (2023). For a stronger theoretical result, we impose a uniform distribution assumption which is also made by Scornet et al. (2015), Wager & Athey (2018) and Blanc et al. (2022). We argue that this uniform distribution assumption is not strong if the splitting variable is continuous as we can convert the variable to its uniformly distributed quantile. Our key assumption on $\eta(x) = P(Y = 1|X = x)$ is that η is continuous with respect to x for any given node t . For Theorem 2.4, we do not require monotonicity of f as in Blanc et al. (2020) or an additive model of f as in Guelman (2012), Scornet et al. (2015), and Klusowski (2021). Furthermore, with the monotonicity assumption, we can attain stronger theoretical results.

Continuous response and treatment effect: Researchers are often interested in continuous outcomes such as sales volume during promotions, milk yield of cows, and patient’s blood glucose level (Ali et al., 2009; Piwczyński et al., 2020; Alexiou et al., 2021). Extending our research to continuous is not trivial as the impurity measure has no closed form like a Bernoulli variable. A special case of continuous outcome is the treatment effect. Policymakers may want to target subpopulations with treatment effects above a certain threshold. Athey & Imbens (2016); Kallus (2017); Wager & Athey (2018); Athey et al. (2019) study treatment effect with regression tree. Integrating our research into their causal inference framework can be an interesting research direction for social scientists, bio-statisticians, and researchers working with causal models.

Representative tree: It is well-known that CART suffers from instability problem (Li & Belford, 2002). As a result, researchers often use random forest or other ensemble methods for prediction. However, this paper focuses on the decision tree for its stellar interpretability. To combine the stability of random forest and interpretability of CART, one should look into representative tree (Sagi & Rokach, 2020; 2021; Gulowaty & Woźniak, 2021). As suggested by its name, the representative tree literature aims to represent a random forest with a single decision tree. An interesting future research direction is to use our method to grow a forest and synthesize a representative tree to output a policy-targeting rule.

Policy learning: (i) The policy learning literature operates under a potential outcome framework and is part of the causal inference literature. LPC problem does not operate under the potential outcome framework, though extending our work to causal inference is undoubtedly interesting for future research as discussed in Appendix A.2, the “continuous response and treatment effect” paragraph.

(ii) The policy learning literature studies treatment assignment optimization problem. While LPC *can* be used for informing treatment assignments, *we do not claim* that our methods optimize the total treatment effects. LPC can also serve other purposes. For example, policymakers can analyze why the identified targeting subpopulations have a higher-than-threshold probability of the binary event and make population-wide policy adjustments or design new policies without prior treatment in mind.

(iii) Our methods do not need a randomized control trial or a quasi-experiment which is a key assumption for the policy learning literature. Experimental data is not always available. For instance, in the case of temporary tax credit programs, it is nearly impossible to conduct an experiment since taxes are collected annually. In such cases, classic policy learning may be impractical, but LPC can help refine policy design by identifying and targeting the subgroups that are more likely financially constrained.

(iv) The criterion function for the policy learning literature is a general welfare criterion defined with respect to treatment effect. We assume a very straightforward thresholding rule as illustrated in the introduction, construct a misclassification risk based on such a rule, and use this risk as the criterion function. The misclassification risk is not a function of the treatment

⁸We do not claim the list to be exhaustive, many important works such as (Breiman, 2001; Biau, 2012; Meinshausen, 2006; Scornet et al., 2015; Wager & Walther, 2015; Zhu et al., 2015; Duan & Xu, 2011; Lin & Jeon, 2006; Mentch & Hooker, 2016; Sexton & Laake, 2009; Efron, 2014) are not included in the list.

effect since there is no treatment in our problem setup.

(v) The theoretical results of the policy learning literature are usually bounds on regret (welfare loss). Since we do not work with welfare function, our theoretical results are with respect to misclassification risk: lower risk under continuity (Theorem 3.1) and optimality under continuity plus monotonicity (Corollary 3.5).

(vi) Our method is computationally much cheaper than those mixed integer programming methods proposed in the policy learning literature. Many empirical studies conducted in the policy learning literature use one or two covariates to decide treatment assignment rules (Kitagawa & Tetenov, 2018; Mbakop & Tabord-Meehan, 2021; Athey & Wager, 2021), our methods can easily accommodate a large number of features as their complexity is the same as constructing CART.

B. Mathematical Appendix

Lemma B.1. *Given the problem setup, for any node t , assume that $\eta(X)$ is continuous and not a constant, $\frac{\partial \mathcal{G}^{CART}(s)}{\partial s} = 0$ is a necessary condition for s to be an optimal split point.*

Proof. We first rule out the possibility that the optimal splitting happens at the boundary point.

Consider $s = 0$, then we write the impurity score as

$$\begin{aligned} \mathcal{G}^{CART}(0) &= (\mu_L(0) - \mu_L^2(0))F(0) + (\mu_R(0) - \mu_R^2(0))(1 - F(0)) \\ &= \mu_R(0) - \mu_R^2(0) = \bar{\eta} - \bar{\eta}^2 \end{aligned}$$

where $\bar{\eta}$ denotes the mean probability of $Y = 1$ for the entire node t .

Since $\eta(X)$ is not a constant, we can find $s = s'$ such that $\mu_L(s') \neq \mu_R(s')$ and in general $\bar{\eta} = \mu_L(s')F(s') + \mu_R(s')(1 - F(s'))$, where $0 < F(s') < 1$. The impurity score for $s = s'$ is

$$\mathcal{G}^{CART}(s') = (\mu_L(s') - \mu_L^2(s'))F(s') + (\mu_R(s') - \mu_R^2(s'))(1 - F(s'))$$

Using the equality $\bar{\eta} = \mu_L(s')F(s') + \mu_R(s')(1 - F(s'))$, we can rewrite $\mathcal{G}(0)$ and show that it is strictly greater than $\mathcal{G}(s')$.

$$\begin{aligned} \mathcal{G}^{CART}(0) &= \mu_L(s')F(s') + \mu_R(s')(1 - F(s')) - (\mu_L(s')F(s') + \mu_R(s')(1 - F(s')))^2 \\ &= \mu_L(s')F(s') + \mu_R(s')(1 - F(s')) - (\mu_L(s')F(s'))^2 - ((\mu_R(s')(1 - F(s'))))^2 \\ &\quad - 2(\mu_L(s')F(s'))(\mu_R(s')(1 - F(s'))) \\ &= \mu_L(s')F(s') + \mu_R(s')(1 - F(s')) - (\mu_L(s')F(s'))^2 - ((\mu_R(s')(1 - F(s'))))^2 \\ &\quad - \mu_L^2(s')F(s')(1 - F(s')) - \mu_R^2(s')F(s')(1 - F(s')) \\ &\quad + \mu_L^2(s')F(s')(1 - F(s')) + \mu_R^2(s')F(s')(1 - F(s')) \\ &\quad - 2(\mu_L(s')F(s'))(\mu_R(s')(1 - F(s'))) \\ &= \mathcal{G}^{CART}(s') + \mu_L^2(s')F(s')(1 - F(s')) + \mu_R^2(s')F(s')(1 - F(s')) \\ &\quad - 2(\mu_L(s')F(s'))(\mu_R(s')(1 - F(s'))) \\ &= \mathcal{G}^{CART}(s') + (\mu_L(s') - \mu_R(s'))^2 F(s')(1 - F(s')) > \mathcal{G}(s') \end{aligned}$$

The inequality means that $s = 0$ can never be the optimal split. The proof for the case of $s = 1$ is similar. Hence, we show that the optimal split is not the boundary point.

Given that $\mathcal{G}^{CART}(s)$ is differentiable, its domain is closed and compact, and the boundary points are not the optimal splits. The first-order condition must be satisfied at all interior local optima (including the global minimum whose argument is the optimal splitting).

□

B.1. Proof for Lemma 2.1

Proof. For a fixed $s \in [0, 1]$, the impurity score after the split is given as:

$$\begin{aligned}\mathcal{G}^{CART}(s) &= (\mu_L - \mu_L^2)F(s) + (\mu_R - \mu_R^2)(1 - F(s)) \\ &= E_t - \mu_L^2 F(s) - \mu_R^2 (1 - F(s)),\end{aligned}\quad (15)$$

where $E_t = \int_0^1 \eta(x)f(x)dx$ is free of s . Moreover,

$$\frac{\partial \mu_L}{\partial s} = \frac{\partial \int_0^s \eta(x)f(x)dx / F(s)}{\partial s} = \frac{f(s)}{F(s)} (\eta(s) - \mu_L) \quad (16)$$

$$\frac{\partial \mu_R}{\partial s} = \frac{\partial \int_s^1 \eta(x)f(x)dx / (1 - F(s))}{\partial s} = \frac{f(s)}{1 - F(s)} (-\eta(s) + \mu_R), \quad (17)$$

Using (16) and (17), we simplify the first-order derivative

$$\begin{aligned}\frac{\partial \mathcal{G}^{CART}(s)}{\partial s} &= -2\mu_L F(s) \frac{\partial \mu_L}{\partial s} - \mu_L^2 f(s) - 2\mu_R (1 - F(s)) \frac{\partial \mu_R}{\partial s} + \mu_R^2 f(s) \\ &= f(s) (-2\mu_L (\eta(s) - \mu_L) - \mu_L^2 - 2\mu_R (-\eta(s) + \mu_R) + \mu_R^2) \\ &= f(s) (-2\mu_L \eta(s) + E_{tL}^2 + 2\mu_R \eta(s) - E_{tR}^2) \\ &= f(s) (2\eta(s) - \mu_L - \mu_R) (\mu_R - \mu_L) \\ &\propto (2\eta(s) - \mu_L - \mu_R) (\mu_R - \mu_L).\end{aligned}\quad (18)$$

By Lemma B.1, $\frac{\partial \mathcal{G}^{CART}(s)}{\partial s} = 0$ is a necessary condition for s to be an optimal split point.

Given that f is strictly positive, we have that $\frac{\partial \mathcal{G}^{CART}(s)}{\partial s} = 0$ iff $(2\eta(s) - \mu_L - \mu_R) (\mu_R - \mu_L) = 0$. The next step is to rule out the possibility that $\mu_R - \mu_L = 0$ outputs a local maximum.

$$\begin{aligned}\frac{\partial^2 \mathcal{G}^{CART}(s)}{\partial s^2} &= \underbrace{(2\eta(s) - \mu_L - \mu_R) (\mu_R - \mu_L)}_{=0 \text{ by the first-order condition}} \frac{\partial f(s)}{\partial s} + \frac{\partial (2\eta(s) - \mu_L - \mu_R) (\mu_R - \mu_L)}{\partial s} f(s) \\ &= \frac{\partial (2\eta(s) - \mu_L - \mu_R) (\mu_R - \mu_L)}{\partial s} f(s) \\ &\propto \frac{\partial (2\eta(s) - \mu_L - \mu_R) (\mu_R - \mu_L)}{\partial s}\end{aligned}$$

Consider the second derivative of $\mathcal{G}(s)$ with respect to s with $\mu_L = \mu_R$, by (16) and (17):

$$\begin{aligned}\frac{\partial^2 \mathcal{G}^{CART}(s)}{\partial s^2} &\propto \frac{\partial (2\eta(s) - \mu_L - \mu_R)}{\partial s} \underbrace{(\mu_R - \mu_L)}_{=0} + (2\eta(s) - \mu_L - \mu_R) \left(\frac{\partial \mu_R}{\partial s} - \frac{\partial \mu_L}{\partial s} \right) \\ &\propto (2\eta(s) - \mu_L - \mu_R) \left(-\frac{\eta(s)}{1 - F(s)} + \frac{\mu_R}{(1 - F(s))} - \frac{\eta(s)}{F(s)} + \frac{\mu_L}{F(s)} \right) \\ &= \frac{2\eta(s) - \mu_L - \mu_R}{F(s)(1 - F(s))} (-\eta(s) + \mu_L(1 - F(s)) + \mu_R F(s))\end{aligned}$$

If $\mu_L = \mu_R$,

$$\frac{\partial^2 \mathcal{G}^{CART}(s)}{\partial s^2} \propto (2\eta(s) - \mu_L - \mu_R) (-\eta(s) + \mu_L) = -2(\eta(s) - \mu_L)^2.$$

For s s.t. $2\eta(s, t) - \mu_L - \mu_R \neq 0$ and $\mu_L = \mu_R$, $\frac{\partial \mathcal{G}^{CART}(s)}{\partial s} = 0$ and $\frac{\partial^2 \mathcal{G}^{CART}(s)}{\partial s^2} < 0$: $\mathcal{G}^{CART}(s)$ reaches its local maximum, which cannot be a global minimum. Such s is not the optimal split.

Global minimum must have $(2\eta(s) - \mu_L - \mu_R) (\mu_R - \mu_L) = 0$ and $\mu_R - \mu_L \neq 0$. Therefore, $2\eta(s, t) - \mu_L - \mu_R = 0$ holds for optimal split s in any node t and dimension p . \square

B.2. Proof for Lemma 2.3

Proof. Using Definition 2.2 and contrapositive,

- when $\eta(x) > c$, $\mu_{t(x)}(s') \leq c \implies \mu_{t(x)}(s) \leq c$ and
- when $\eta(x) \leq c$, $\mu_{t(x)}(s') > c \implies \mu_{t(x)}(s) > c$.

Therefore, $\forall x \in [0, 1]$,

$$\begin{aligned} \mathbb{1}\{\eta(x) > c\} \mathbb{1}\{\mu_{t(x)}(s') \leq c\} &\leq \mathbb{1}\{\eta(x) > c\} \mathbb{1}\{\mu_{t(x)}(s) \leq c\} \\ \mathbb{1}\{\eta(x) \leq c\} \mathbb{1}\{\mu_{t(x)}(s') > c\} &\leq \mathbb{1}\{\eta(x) \leq c\} \mathbb{1}\{\mu_{t(x)}(s) > c\} \end{aligned}$$

Also, there exists a set $\mathcal{A} \subseteq [0, 1]$ with nonzero measure such that, $\forall x \in \mathcal{A}$, either (or both) of the following conditions is true

$$\begin{aligned} \mathbb{1}\{\eta(x) > c\} \mathbb{1}\{\mu_{t(x)}(s') \leq c\} &< \mathbb{1}\{\eta(x) > c\} \mathbb{1}\{\mu_{t(x)}(s) \leq c\} \\ \mathbb{1}\{\eta(x) \leq c\} \mathbb{1}\{\mu_{t(x)}(s') > c\} &< \mathbb{1}\{\eta(x) \leq c\} \mathbb{1}\{\mu_{t(x)}(s) > c\} \end{aligned}$$

$$\begin{aligned} R(s') &= \int_{\tilde{X}_t}^{\tilde{X}_t} (\mathbb{1}\{\eta(x) > c\} \mathbb{1}\{\mu_{t(x)}(s') \leq c\} + \mathbb{1}\{\eta(x) \leq c\} \mathbb{1}\{\mu_{t(x)}(s') > c\}) f(x) dx \\ &< \int_{\tilde{X}_t}^{\tilde{X}_t} (\mathbb{1}\{\eta(x) > c\} \mathbb{1}\{\mu_{t(x)}(s) \leq c\} + \mathbb{1}\{\eta(x) \leq c\} \mathbb{1}\{\mu_{t(x)}(s) > c\}) f(x) dx = R_t(s) \end{aligned}$$

□

B.3. Proof for Theorem 2.4

Proof. By Lemma 2.1, without loss of generality⁹, assume

$$\mu_L(s^{CART}) < \eta(s^{CART}) = \frac{\mu_L(s^{CART}) + \mu_R(s^{CART})}{2} < \mu_R(s^{CART}).$$

We sequentially prove the two claims in the lemma: the existence of s^* and risk reduction.

Existence of s^* When $\eta(s^{CART}, t) > c$, we have $(\eta(s^{CART}) - c)(\mu_R(s^{CART}) - \mu_L(s^{CART})) > 0$, so we want to show that $\exists s \in (0, s^{CART})$ such that $\eta(s) = c$.

$$\mu_L = \min(\mu_L, \mu_R) \leq c \implies \exists \tilde{s} \in [0, s^{CART}] \text{ such that } \eta(\tilde{s}) \leq c$$

If $\eta(\tilde{s}) = c$, then the existence of s^* is proven. If $\eta(\tilde{s}) < c$, then by intermediate value theorem, $\exists s \in (\tilde{s}, s^{CART})$ such that $\eta(s) = c$, the proof for existence of s^* is complete for $\eta(s^{CART}, t) > c$. The case when $\eta(s^{CART}, t) \leq c$ can be proved using the same logic.

We showed that when $\eta(s^{CART}, t) > c$, there exists s^* and the s^* is in the range $(0, s^{CART})$. By continuity of η and the definition of s^* , $\forall s \in (s^*, s^{CART}), \eta(s) > c$. By the same logic, we have that when $\eta(s^{CART}, t) \leq c$, $\forall s \in (s^{CART}, s^*), \eta(s) \leq c$.

Risk reduction We compare risks led by s^{CART} and s^* :

⁹Proof for the case $\mu_R(s^{CART}) < \eta(s^{CART}) < \mu_L(s^{CART})$ is similar.

1. If $\eta(s^{CART}) \leq c$, for any $s \in (s^{CART}, s^*)$, we have $\eta(s) \leq c$ and

$$\begin{aligned}\mu_L(s) &= \int_0^s \eta(x)f(x)dx/F(s) = \frac{\int_0^{s^{CART}} \eta(x)f(x)dx + \int_{s^{CART}}^{s^*} \eta(x)f(x)dx}{F(s)} \\ &< \frac{\int_0^{s^{CART}} \eta(x)f(x)dx + c \int_{s^{CART}}^{s^*} f(x)dx}{F(s)} = \frac{\mu_L(s^{CART})F(s^{CART}) + c(F(s) - F(s^{CART}))}{F(s)} < c \\ \mu_R(s) &> \frac{\mu_R(s^{CART})(1 - F(s^{CART})) - c(F(s) - F(s^{CART}))}{1 - F(s)} > c.\end{aligned}$$

Since the order that $\mu_L(s) \leq c < \mu_R(s)$ does not change and $\forall s \in (s^{CART}, s^*), \eta(s) \leq c$, we have that when $X \in [0, s^{CART}]$, splitting rules s and s^{CART} are equivalent in classifying the latent probability; when $X \in (s^{CART}, s)$ which has a nonzero measure, splitting rule s performs strictly better than s^{CART} in classifying the latent probability; when $X \in [s, 1]$, splitting rules s and s^{CART} are equivalent in classifying the latent probability. Therefore, s strictly dominates s^{CART} .

$$R(s^{CART}) - R(s) = (F(s) - F(s^{CART})) > 0,$$

which is continuously monotone decreasing with respect to s by the assumption that $f > 0$, where f is the pdf of X .

2. If $\eta(s^{CART}) > c$, for $s \in (s^*, s^{CART})$, we have $\eta(s) > c$, s strictly dominates s^{CART} , and

$$R(s^{CART}) - R(s) = (F(s^{CART}) - F(s)) > 0,$$

which is continuously monotone increasing with respect to s by the assumption that $f > 0$. □

B.4. Proof for Theorem 3.1

Proof. Consider

$$\frac{\partial \mathcal{G}^{PFS}(s, c)}{\partial s} = \frac{\partial \mathcal{G}^{CART}(s, c) + \lambda W(|\mu_L - c|)F(s) + \lambda W(|\mu_R - c|)(1 - F(s))}{\partial s}.$$

We focus on the new term $\frac{\partial W(|\mu_L - c|)F(s)}{\partial s}$ and $\frac{\partial W(|\mu_R - c|)(1 - F(s))}{\partial s}$. By (16) and (17),

$$\begin{aligned}\frac{\partial W(|\mu_L - c|)F(s)}{\partial s} &= f(s)W(|\mu_L - c|) + \frac{\partial W(|\mu_L - c|)}{\partial \mu_L} \frac{\partial \mu_L}{\partial s} F(s) \\ &= f(s) \left(W(|\mu_L - c|) + \frac{\partial W(|\mu_L - c|)}{\partial \mu_L} (\eta(s) - \mu_L) \right) \\ \frac{\partial W(|\mu_R - c|)(1 - F(s))}{\partial s} &= -f(s)W(|\mu_R - c|) + \frac{\partial W(|\mu_R - c|)}{\partial \mu_R} \frac{\partial \mu_R}{\partial s} (1 - F(s)) \\ &= f(s) \left(-W(|\mu_R - c|) + \frac{\partial W(|\mu_R - c|)}{\partial \mu_R} (\mu_R - \eta(s)) \right).\end{aligned}$$

With $\mathcal{G}^{PFS}(s, c)$'s derivative with respect to s , we evaluate how $\frac{\partial \mathcal{G}^{PFS}(s, c)}{\partial s}$ behaves at s^{CART} , i.e., when $2\eta(s) - \mu_L - \mu_R = 0$ and at s^* , i.e., when $\eta(s) = c$ respectively:

$$\begin{aligned}\frac{1}{\lambda f(s)} \frac{\partial \mathcal{G}^{PFS}(s, c)}{\partial s} \Big|_{s=s^{CART}} &= W(|\mu_L - c|) - W(|\mu_R - c|) \\ &\quad + \left(\frac{\partial W(|\mu_L - c|)}{\partial \mu_L} + \frac{\partial W(|\mu_R - c|)}{\partial \mu_R} \right) (\eta(s^{CART}) - \mu_L)\end{aligned}\tag{19}$$

$$\begin{aligned}\frac{1}{f(s)} \frac{\partial \mathcal{G}^{PFS}(s, c)}{\partial s} \Big|_{s=s^*} &= (2c - \mu_L - \mu_R)(\mu_R - \mu_L) + \lambda(W(|\mu_L - c|) - W(|\mu_R - c|)) \\ &\quad + \lambda \left(\frac{\partial W(|\mu_L - c|)}{\partial \mu_L} (c - \mu_L) + \frac{\partial W(|\mu_R - c|)}{\partial \mu_R} (\mu_R - c) \right).\end{aligned}\tag{20}$$

Note that s^* in (20) is only guaranteed to exist when the condition of c in Theorem 2.4 is met. We will address this in the latter part of the proof. Next, consider all five possible scenarios of c 's location separately. (Still, without loss of generality, assume $\mu_L(s^{CART}) < \eta(s^{CART}) < \mu_R(s^{CART})$.)

i. $\mu_L(s^{CART}) \leq c < \eta(s^{CART}) < \mu_R(s^{CART})$.

By Lemma 2.1, $|\mu_R(s^{CART}) - c| > |\mu_L(s^{CART}) - c|$. $W(|\mu_L - c|) > W(|\mu_R - c|)$ by the monotonicity of W and $\frac{\partial W(|\mu_L - c|)}{\partial \mu_L} + \frac{\partial W(|\mu_R - c|)}{\partial \mu_R} \geq 0$ by the convexity of W . Thus, by (19),

$$\left. \frac{\partial \mathcal{G}^{PFS}(s, c)}{\partial s} \right|_{s=s^{CART}} > 0. \quad (21)$$

By Lemma 2.1, and continuity of η , μ_L and μ_R ,

$$(2\eta(s) - \mu_L - \mu_R)(\mu_R - \mu_L) < 0, \quad s \in (s^{sp}, s^{CART}),$$

where $s^{sp} := \max\{s : s < s^{CART}, (2\eta(s) - \mu_L - \mu_R)(\mu_R - \mu_L) = 0\}$. If there is no such $s^{sp} > 0$ exists, let $s^{sp} = 0$. When $s \in (\max\{s^*, s^{sp}\}, s^{CART})$, by Theorem 2.4, $\mu_L < c$ and $\mu_R > c$.

When $s^* > s^{sp}$, define $d_L := c - \mu_L$ and $d_R := \mu_R - c$ and we have

$$0 > (2c - \mu_L(s^*) - \mu_R(s^*))(\mu_R(s^*) - \mu_L(s^*)) = (d_L - d_R)(d_L + d_R),$$

which directly suggests that $d_L < d_R$. Let $W_2(d) = d^2 + \lambda(W(d) - dW'(d))$. We can rewrite (20) as:

$$\begin{aligned} \frac{1}{f(s)} \left. \frac{\partial \mathcal{G}^{PFS}(s, c)}{\partial s} \right|_{s=s^*} &= d_L^2 + \lambda \left(W(d_L) - d_L \frac{\partial W(d_L)}{\partial d_L} \right) - d_R^2 - \lambda \left(W(d_R) - d_R \frac{\partial W(d_R)}{\partial d_R} \right) \\ &= W_2(d_L) - W_2(d_R). \end{aligned}$$

Note that $W_2'(d) = d(2 - \lambda W''(d))$. By the bounded second derivative assumption, set $\Lambda_1 = \frac{1}{\max\{W''(d_L), W''(d_R)\}}$. Since $0 < d_L < d_R$, when $\lambda < \Lambda_1$, $W_2(d_L) < W_2(d_R)$,

$$\frac{1}{f(s)} \left. \frac{\partial \mathcal{G}^{PFS}(s, c)}{\partial s} \right|_{s=s^*} < 0.$$

When $s^* < s^{sp}$, there exists $s^{in} \in (s^{sp}, s^{CART})$ and $c > 0$ s.t.

$$(2\eta(s) - \mu_L - \mu_R)(\mu_R - \mu_L) < -c,$$

by unique global minimum assumption and continuity. With $\Lambda_1 = \frac{c}{W(0) + W'(0)}$, we have

$$\frac{1}{f(s)} \left. \frac{\partial \mathcal{G}^{PFS}(s, c)}{\partial s} \right|_{s=s^{in}} < 0.$$

Thus, for $0 < \lambda < \Lambda_1$, there exists a $s \in [s^*, s^{CART})$ s.t.

$$\frac{\partial \mathcal{G}^{PFS}(s, c)}{\partial s} < 0. \quad (22)$$

Considering (21) and (22) jointly with the continuity of the derivative, we can conclude that there exists a $s^{**} \in (s^*, s^{CART})$ such that $\left. \frac{\partial \mathcal{G}^{PFS}(s, c)}{\partial s} \right|_{s=s^{**}} = 0$. s^{**} is a local minimizer of $\mathcal{G}^{PFS}(s, c)$ and is guaranteed to give a smaller risk than s^{CART} by Theorem 2.4.

Next, we argue that with some additional bound for λ , s^{**} is also the global optimal split under the penalized impurity measure. To simplify the notation in the rest of the proof, let s^{in} be s^* if $s^* < s^{sp}$. Then, we want to show $\mathcal{G}^{PFS}(s^{**}, c) < \mathcal{G}^{PFS}(s, c)$ for $s \neq s^{**}$:

(a). Consider s such that there is at least one s^{sp} in between s and s^{**} . By unique optimizer assumption for G , if there is more than one local minimum, i.e., multiple s that have $2\eta(s, t) - \mu_L - \mu_R = 0$, we assume the global minimum and the second smallest local minimum, gives by s^{sc} , different by Δ . Let $\Lambda_2 = \frac{\Delta}{W(0) - \min(W(c), W(1-c))}$. For $0 < \lambda < \Lambda_2$,

$$\begin{aligned} \mathcal{G}^{PFS}(s^{**}, c) &< \mathcal{G}^{PFS}(s^{CART}, c) \\ &= \mathcal{G}(s^{CART}, c) + \lambda(W(|\mu_L - c|)F(s) + W(|\mu_R - c|)(1 - F(s))) \\ &\leq \mathcal{G}(s^{CART}, c) + \lambda W(0) \\ &\leq \mathcal{G}(s^{sc}, c) + \lambda \min\{W(c), W(1-c)\} \leq \mathcal{G}^{PFS}(s, c) \end{aligned}$$

(b). Consider s such that there is no s^{sp} in between s and s^{**} .

When $s \in (s^*, s^{CART})$, $\mathcal{G}^{PFS}(s^{**}, c) < \mathcal{G}^{PFS}(s, c)$ by definition.

When $s < s^*$, by (22) and continuity of $\frac{\partial \mathcal{G}^{PFS}(s, c)}{\partial s}$, there can be two possible scenarios. One, there exist a $s_0 < s^*$ such that $\frac{\partial \mathcal{G}^{PFS}(s, c)}{\partial s} = 0$ and $\mathcal{G}^{PFS}(s_0, c) - \mathcal{G}^{PFS}(s^{**}, c) := \Delta_L > 0$. Then, define $\Lambda_3 = \frac{\Delta_L}{W(0) - \min(W(c), W(1-c))}$. For $0 < \lambda < \Lambda_3$, $\mathcal{G}^{PFS}(s^{**}, c) < \mathcal{G}^{PFS}(s, c)$ when $s_0 \leq s < s^*$ by definition. When $s < s_0$:

$$\begin{aligned} \mathcal{G}^{PFS}(s^{**}, c) &= \mathcal{G}^{PFS}(s_0, c) - \Delta_L \\ &= \mathcal{G}(s_0, c) + \lambda(W(|\mu_L - c|)F(s) + W(|\mu_R - c|)(1 - F(s))) - \Delta_L \\ &\leq \mathcal{G}(s_0, c) + \lambda W(0) - \Delta_L \\ &\leq \mathcal{G}(s_0, c) + \lambda \min\{W(c), W(1-c)\} \\ &\leq \mathcal{G}(s, c) + \lambda(W(|\mu_L - c|)F(s) + W(|\mu_R - c|)(1 - F(s))) = \mathcal{G}^{PFS}(s, c). \end{aligned}$$

Two, $\frac{\partial \mathcal{G}^{PFS}(s, c)}{\partial s} < 0$. Then $\mathcal{G}^{PFS}(s^{**}, c) < \mathcal{G}^{PFS}(s, c)$ for $s < s^*$ follows.

When $s > s^{CART}$, we can follow the same procedure as when $s < s^*$. If there exists a $s_1 > s^*$ such that $\frac{\partial \mathcal{G}^{PFS}(s, c)}{\partial s} = 0$ and $\mathcal{G}^{PFS}(s_1, c) - \mathcal{G}^{PFS}(s^{**}, c) := \Delta_R > 0$. We can define $\Lambda_4 = \frac{\Delta_R}{W(0) - \min(W(c), W(1-c))}$ and everything else follows.

To conclude, for $0 < \lambda \leq \Lambda = \min\{\Lambda_1, \Lambda_2, \Lambda_3, \Lambda_4\}$, the theoretical optimal split chosen with respect to G^{PFS} leads to a risk smaller than s^{CART} when $\mu_L(s^{CART}) \leq c < \eta(s^{CART}) < \mu_R(s^{CART})$.

ii. $\mu_L(s^{CART}) < \eta(s^{CART}) < c \leq \mu_R(s^{CART})$. This scenario is symmetric to **i** and is also considered in Theorem 2.4. It can be proved following the same logic as in **i**.

iii. $c < \mu_L(s^{CART}) < \eta(s^{CART}) < \mu_R(s^{CART})$.

In this scenario, consider two split points located on each side of s^{CART} respectively: let s_{c1} be the largest split less than s^{CART} such that $\mu_L(s_{c1}) = c$, s_{c2} be the smallest split greater than s^{CART} such that $\mu_L(s_{c2}) = c$, s_L be the largest split less than s^{CART} such that $\eta(s_L) \geq \mu_L(s^{CART})$ and s_R be the smallest split greater than s^{CART} such that $\eta(s_R) = \mu_R(s^{CART})$. Let $s_{c1} = 0$ or $s_{c2} = 1$ if no such s_{c1} or s_{c2} exists. Both s_L and s_R 's existence is guaranteed by the intermediate value theorem which we used once in Theorem 2.4.

We argue for any $s \in (\max(s_L, s_{c1}), \min(s_R, s_{c2}))$, risk is no greater than s^{CART} .

For $s \in (\max(s_L, s_{c1}), s^{CART})$, it is a piece of x that has $\eta(x) > \mu_L(s^{CART})$ being split to right.

$$\begin{aligned} \mu_R(s) &> \frac{\mu_R(s^{CART})(1 - F(s^{CART})) + \mu_L(s^{CART})(F(s^{CART}) - F(s))}{1 - F(s)} > \mu_L(s^{CART}) > c \\ c < \mu_L(s) &< \frac{\mu_L(s^{CART})F(s^{CART}) - \mu_L(s^{CART})(F(s^{CART}) - F(s))}{F(s)} = \mu_L(s^{CART}). \end{aligned}$$

Since $c < \mu_L(s) < \mu_L(s^{CART}) < \mu_R(s)$, the expectations on both sides remain greater than c and the risk is the same as split s^{CART} . When $s \in (s^{CART}, \min(s_R, s_{c2}))$, $c < \mu_L(s) < \mu_R(s^{CART}) < \mu_R(s)$ can be obtained similarly and the risk also remains.

Note that $\mu_R(s) > \mu_L(s)$ all the way when $s \in (\max(s_L, s_{c1}), \min(s_R, s_{c2}))$. We can then define Δ the same as in scenario **i**, $\Delta_L = \mathcal{G}^{PFS}(\max(s_L, s_{c1}), c)$, and $\Delta_R = \mathcal{G}^{PFS}(\min(s_R, s_{c2}), c)$. $\Lambda_2, \Lambda_3, \Lambda_4$ are defined accordingly. For $0 < \lambda \leq \Lambda = \min\{\Lambda_2, \Lambda_3, \Lambda_4\}$, the theoretical optimal split chosen with respect to G^{PFS} leads to the same risk as s^{CART} when $c < \mu_L(s^{CART}) < \eta(s^{CART}) < \mu_R(s^{CART})$.

iv. $\mu_L(s^{CART}) < \eta(s^{CART}) < \mu_R(s^{CART}) < c$. This scenario is symmetric to **iii**. It can be proved following the same logic in **iii**.

v. $\mu_L(s^{CART}) < \eta(s^{CART}) = c < \mu_R(s^{CART})$. This scenario can be considered a special case of **i** and **ii**. By appropriate choice of Λ , it's trivial to show that the original s^{CART} remains the global optimizer and the risk stays the same. □

We find it clearer to prove Corollary 3.5 and then plug in some of the steps in the proof for Corollary 3.5 into proof for Theorem 3.4. Hence, we first present the proof for Corollary 3.5.

B.5. Proof for Corollary 3.5

Proof. WLOG, assume η is monotonically increasing with respect to x . The proof for the monotonically decreasing case is similar. We will first discuss two distinct cases: $\mu_L < \mu_R \leq c$ and $c \leq \mu_L < \mu_R$ and show that for both cases \mathcal{G}^* is constant. Then, we consider the case where $\mu_L \leq c \leq \mu_R$ and show that s^* maximizes \mathcal{G}^* in this case. We complete the proof by showing that $\mathcal{G}^*(s^*, c)$ is larger than the two constant \mathcal{G}^* for the first two cases.

i. $\mu_L < \mu_R \leq c$, we can write \mathcal{G}^* as

$$s \left(c - \frac{\int_0^s \eta(x) dx}{s} \right) + (1-s) \left(c - \frac{\int_s^1 \eta(x) dx}{1-s} \right) = c - \int_0^1 \eta(x) dx$$

Note that in this case, \mathcal{G}^* is a constant.

ii. $c \leq \mu_L < \mu_R$, we can write \mathcal{G}^* as

$$s \left(\frac{\int_0^s \eta(x) dx}{s} - c \right) + (1-s) \left(\frac{\int_s^1 \eta(x) dx}{1-s} - c \right) = \int_0^1 \eta(x) dx - c$$

Note that in this case, \mathcal{G}^* is a constant.

iii. $\mu_L \leq c \leq \mu_R$, we can write $\max_s \mathcal{G}^*$ as

$$\max_s s \left(c - \frac{\int_0^s \eta(x) dx}{s} \right) + (1-s) \left(\frac{\int_s^1 \eta(x) dx}{1-s} - c \right)$$

The first-order condition is $c - \eta(s) - \eta(s) + c = 0$. We solve $\eta(s) = c$, hence, s^* is a local optima. Moreover, second order derivative is $-2\eta'(s^*)$ which is negative given that η is strictly increasing and differentiable in a neighborhood of s^* . Hence, s^* is a local maxima. Since \mathcal{G}^* is continuous in s , we need to show that $\mathcal{G}^*(s^*)$ is larger than the boundary points for the case $\mu_L \leq c \leq \mu_R$ to claim s^* as the global maxima for case iii. There are two possibilities for the boundary points

Possibility 1: Consider s_1 and s_2 and their associated $\mathcal{G}^*(s_1)$ and $\mathcal{G}^*(s_2)$ where $\mu_L(s_1) = c$ and $\mu_R(s_2) = c$. Since s_1 is included in case ii; whereas s_2 is included in case i, once we show that $\mathcal{G}^*(s^*) > \mathcal{G}^*(s_1), \mathcal{G}^*(s_2)$, we can claim s^* to be the unique global maxima among all possible s .

$$\begin{aligned}
 \mathcal{G}^*(s^*) &= s^*c - \int_0^{s^*} \eta(x)dx + \int_{s^*}^1 \eta(x)dx - (1 - s^*)c \\
 &> s^*c - \int_0^{s^*} \eta(x)dx + (1 - s^*)c - \int_{s^*}^1 \eta(x)dx \\
 &= c - \int_0^1 \eta(x)dx = \mathcal{G}^*(s_2) \\
 \mathcal{G}^*(s^*) &= s^*c - \int_0^{s^*} \eta(x)dx + \int_{s^*}^1 \eta(x)dx - (1 - s^*)c \\
 &> \int_0^{s^*} \eta(x)dx - s^*c + (1 - s^*)c - (1 - s^*)c \\
 &= \int_0^1 \eta(x)dx - c = \mathcal{G}^*(s_1)
 \end{aligned}$$

Possibility 2: Even at the boundary point, $\mu_L \leq c \leq \mu_R$ still holds. Then, the boundary points for case iii are $s = 0$ and $s = 1$.

$$\begin{aligned}
 \tilde{G}(0) &= \int_0^1 \eta(x)dx - c < \mathcal{G}^*(s^*) \\
 \tilde{G}(1) &= c - \int_0^1 \eta(x)dx < \mathcal{G}^*(s^*)
 \end{aligned}$$

Since under Possibility 2 case iii spans the entire domain of X , s^* is the unique global maxima. Note that Assumption 3.3 implies that $\exists \epsilon > 0$, such that $s^* \in [\epsilon, 1 - \epsilon] \subset [0, 1]$. Therefore, s^* is the global maxima among all possible s . \square

B.6. Proof for Theorem 3.4

Proof. Again, assume that η is monotonically increasing in the neighborhood of s^* , the proof for the monotonically decreasing case is the same. Assumption 3.3 guarantees $\forall s < s^*, \eta(X) < c, \forall s > s^*, \eta(X) > c$.

Let $[s^* - \epsilon_1, s^* + \epsilon_1]$ denote the monotonically increasing η neighborhood of s^* , where $\epsilon_1 > 0$. Let $[s^* - \epsilon_2, s^* + \epsilon_2]$ denote an interval that contains s^* in which $\forall s \in [s^* - \epsilon_2, s^* + \epsilon_2], \mu_L < c < \mu_R$ and $\epsilon_2 > 0$. The existence of $[s^* - \epsilon_2, s^* + \epsilon_2]$ is guaranteed because both μ_L and μ_R are continuous in s and given Assumption 3.3, $\mu_L(s^*) < c < \mu_R(s^*)$.

Consider $s \in [s^* - \epsilon_1, s^* + \epsilon_1] \cap [s^* - \epsilon_2, s^* + \epsilon_2] = [a, b]$, where $a = \max(s^* - \epsilon_1, s^* - \epsilon_2)$ and $b = \min(s^* + \epsilon_1, s^* + \epsilon_2)$. This case is equivalent to case iii in the proof for Corollary 3.5. Hence, s^* is a local maxima for the interval $[a, b]$ and \mathcal{G}^* is

$$s^*c - \int_0^{s^*} \eta(x)dx + \int_{s^*}^1 \eta(x)dx - (1 - s^*)c.$$

Consider $s \leq a$. When $\mu_R \leq c$, \mathcal{G}^* is $c - \int_0^1 \eta(x)dx$, the proof is identical to case i in the proof for Corollary 3.5. When $\mu_R > c$,

$$\begin{aligned}
 \mathcal{G}^* &= sc - \int_0^s \eta(x)dx + \int_s^1 \eta(x)dx - (1 - s)c \\
 &= sc + \int_s^{s^*} \eta(x)dx - \int_0^{s^*} \eta(x)dx + \int_{s^*}^1 \eta(x)dx + \int_s^{s^*} \eta(x)dx - (1 - s)c \\
 &< sc + (s^* - s)c - \int_0^{s^*} \eta(x)dx + \int_{s^*}^1 \eta(x)dx + (s^* - s)c - (1 - s)c \\
 &= s^*c - \int_0^{s^*} \eta(x)dx + \int_{s^*}^1 \eta(x)dx - (1 - s^*)c
 \end{aligned}$$

The proof for when $s \geq b$ is similar, those s results in higher \mathcal{G}^* .

Since s^* is the unique point in the interval $[a, b]$ which meets the first-order condition and the boundary points $\{a, b\}$ have lower \mathcal{G}^* than s^* , s^* is the unique maxima in the interval $[a, b]$. Moreover, $s \in [0, a] \cup [b, 1]$ also have lower \mathcal{G}^* than s^* , hence, s^* is the unique global maxima. \square

B.7. Proof for Theorem 4.1

Proof. Outline: We leverage tools for studying asymptotic properties of M-estimator. To show $\hat{s} \xrightarrow{P} s^*$, we take two steps:

1. Under Assumption 3.3, we show uniform convergence of the estimator of cost function $\hat{\mathcal{G}}^*$ to its population target \mathcal{G}^* , i.e., $\sup_{s \in (\epsilon, 1-\epsilon)} |\mathcal{G}^*(s, c) - \hat{\mathcal{G}}^*(s, c)| \xrightarrow{P} 0$ as $n \rightarrow \infty$.
2. Combining with Theorem 3.4, we can apply Theorem 5.7 of Van der Vaart (2000) and get the desired result.

Step 1. For any given $c \in (0, 1)$ and $\epsilon_0 > 0$, we have

$$\begin{aligned} & \mathbb{P} \left(\sup_{s \in (\epsilon, 1-\epsilon)} |\mathcal{G}^*(s, c) - \hat{\mathcal{G}}^*(s, c)| \geq \epsilon_0 \right) \\ &= \mathbb{P} \left(\sup_{s \in (\epsilon, 1-\epsilon)} \left| s \left| \frac{\sum_{i=1}^n Y_i \mathbb{1}\{X_i \leq s\}}{\sum_{i=1}^n \mathbb{1}\{X_i \leq s\}} - c \right| - s|\mu_L - c| \right. \right. \\ & \quad \left. \left. + (1-s) \left| \frac{\sum_{i=1}^n Y_i \mathbb{1}\{X_i > s\}}{\sum_{i=1}^n \mathbb{1}\{X_i > s\}} - c \right| - (1-s)|\mu_R - c| \right| \geq \epsilon_0 \right) \\ &\leq \mathbb{P} \left(\sup_{s \in (\epsilon, 1-\epsilon)} s \left| \frac{\sum_{i=1}^n Y_i \mathbb{1}\{X_i \leq s\}}{\sum_{i=1}^n \mathbb{1}\{X_i \leq s\}} - \mu_L \right| \geq \epsilon_0/2 \right) \end{aligned} \quad (23)$$

$$+ \mathbb{P} \left(\sup_{s \in (\epsilon, 1-\epsilon)} (1-s) \left| \frac{\sum_{i=1}^n Y_i \mathbb{1}\{X_i > s\}}{\sum_{i=1}^n \mathbb{1}\{X_i > s\}} - \mu_R \right| \geq \epsilon_0/2 \right) \quad (24)$$

We focus on showing (23) goes to 0 as $n \rightarrow \infty$, the proof for (24) is exactly the same.

For any $\delta > 0$, denote event $\mathcal{E} = \inf_{s \in (\epsilon, 1-\epsilon)} n^{-1} \sum_{i=1}^n \mathbb{1}\{X_i \leq s\} \geq \delta$. We have

$$\begin{aligned} & \mathbb{P} \left(\sup_{s \in (\epsilon, 1-\epsilon)} s \left| \frac{\sum_{i=1}^n Y_i \mathbb{1}\{X_i \leq s\}}{\sum_{i=1}^n \mathbb{1}\{X_i \leq s\}} - \mu_L \right| \geq \epsilon_0/2 \right) \\ &\leq \mathbb{P} \left(\sup_{s \in (\epsilon, 1-\epsilon)} s \left(\frac{|n^{-1} \sum_{i=1}^n Y_i \mathbb{1}\{X_i \leq s\} - s\mu_L|}{n^{-1} \sum_{i=1}^n \mathbb{1}\{X_i \leq s\}} + \frac{\mu_L |n^{-1} \sum_{i=1}^n \mathbb{1}\{X_i \leq s\} - s|}{n^{-1} \sum_{i=1}^n \mathbb{1}\{X_i \leq s\}} \right) \geq \epsilon_0/2 \right) \\ &\leq \mathbb{P} \left(\sup_{s \in (\epsilon, 1-\epsilon)} \frac{s |n^{-1} \sum_{i=1}^n Y_i \mathbb{1}\{X_i \leq s\} - s\mu_L|}{n^{-1} \sum_{i=1}^n \mathbb{1}\{X_i \leq s\}} \geq \epsilon_0/4 \right) + \mathbb{P} \left(\sup_{s \in (\epsilon, 1-\epsilon)} \frac{\mu_L |n^{-1} \sum_{i=1}^n \mathbb{1}\{X_i \leq s\} - s|}{n^{-1} \sum_{i=1}^n \mathbb{1}\{X_i \leq s\}} \geq \epsilon_0/4 \right) \\ &\leq \mathbb{P} \left(\frac{\sup_{s \in (\epsilon, 1-\epsilon)} s |n^{-1} \sum_{i=1}^n Y_i \mathbb{1}\{X_i \leq s\} - s\mu_L|}{\inf_{s \in (\epsilon, 1-\epsilon)} n^{-1} \sum_{i=1}^n \mathbb{1}\{X_i \leq s\}} \geq \epsilon_0/4 \right) + \mathbb{P} \left(\frac{\sup_{s \in (\epsilon, 1-\epsilon)} \mu_L |n^{-1} \sum_{i=1}^n \mathbb{1}\{X_i \leq s\} - s|}{\inf_{s \in (\epsilon, 1-\epsilon)} n^{-1} \sum_{i=1}^n \mathbb{1}\{X_i \leq s\}} \geq \epsilon_0/4 \right) \\ &\leq \mathbb{P} \left(\sup_{s \in (\epsilon, 1-\epsilon)} s \left| n^{-1} \sum_{i=1}^n Y_i \mathbb{1}\{X_i \leq s\} - s\mu_L \right| \geq (\epsilon_0\delta)/4, \mathcal{E} \right) + \mathbb{P} \left(\sup_{s \in (\epsilon, 1-\epsilon)} \mu_L \left| n^{-1} \sum_{i=1}^n \mathbb{1}\{X_i \leq s\} - s \right| \geq (\epsilon_0\delta)/4, \mathcal{E} \right) \\ &\leq \mathbb{P} \left(\sup_{s \in (\epsilon, 1-\epsilon)} s \left| n^{-1} \sum_{i=1}^n Y_i \mathbb{1}\{X_i \leq s\} - s\mu_L \right| \geq (\epsilon_0\delta)/4 \right) \end{aligned} \quad (25)$$

$$+ \mathbb{P} \left(\sup_{s \in (\epsilon, 1-\epsilon)} \mu_L \left| n^{-1} \sum_{i=1}^n \mathbb{1}\{X_i \leq s\} - s \right| \geq (\epsilon_0\delta)/4 \right) \quad (26)$$

For (25), let $\mathbf{Z}_i = (X_i, Y_i)$, $i = 1, \dots, n$ and $f(\mathbf{Z}_i, s) = Y_i \mathbb{1}_{\{X_i \leq s\}}$. Notice $\mathbb{E}[f(\mathbf{Z}, s)] = s\mu_L$, $f(\mathbf{Z}, s)$ is continuous at each $s \in (0, 1)$ for almost all \mathbf{Z} , since discontinuity occurs at $X_i = s$, which has measure zero for $X_i \sim \text{Unif}(0, 1)$. Also, $f(\mathbf{Z}, s) \leq \mathbb{1}_{\{0 \leq X \leq 1\}}$ with $\mathbb{E}[\mathbb{1}_{\{0 \leq X \leq 1\}}] = 1 \leq \infty$. Applying uniform law of large numbers, we know

$$\begin{aligned} & \mathbb{P}\left(\sup_{s \in (\epsilon, 1-\epsilon)} s \left| n^{-1} \sum_{i=1}^n Y_i \mathbb{1}_{\{X_i \leq s\}} - s\mu_L \right| \geq (\epsilon_0 \delta)/4\right) \\ & \leq \mathbb{P}\left(\sup_{s \in (\epsilon, 1-\epsilon)} \left| n^{-1} \sum_{i=1}^n Y_i \mathbb{1}_{\{X_i \leq s\}} - s\mu_L \right| \geq (\epsilon_0 \delta)/4\right) \\ & \leq \mathbb{P}\left(\sup_{s \in (0, 1)} \left| n^{-1} \sum_{i=1}^n Y_i \mathbb{1}_{\{X_i \leq s\}} - s\mu_L \right| \geq (\epsilon_0 \delta)/4\right) \rightarrow 0, \end{aligned} \quad (27)$$

as $n \rightarrow \infty$. For (26), notice $F_n(s) = n^{-1} \sum_{i=1}^n \mathbb{1}_{\{X_i \leq s\}}$ is the empirical CDF of $X \sim \text{Unif}(0, 1)$, with CDF $F_X(s) = s$ for $s \in (0, 1)$. Applying Dvoretzky–Kiefer–Wolfowitz inequality, we have

$$\begin{aligned} & \mathbb{P}\left(\sup_{s \in (\epsilon, 1-\epsilon)} \left| \mu_L n^{-1} \sum_{i=1}^n \mathbb{1}_{\{X_i \leq s\}} - s \right| \geq (\epsilon_0 \delta)/4\right) \\ (\mu_L \in [0, 1]) & \leq \mathbb{P}\left(\sup_{s \in (\epsilon, 1-\epsilon)} \left| n^{-1} \sum_{i=1}^n \mathbb{1}_{\{X_i \leq s\}} - s \right| \geq (\epsilon_0 \delta)/4\right) \\ & \leq \mathbb{P}\left(\sup_{s \in (0, 1)} \left| n^{-1} \sum_{i=1}^n \mathbb{1}_{\{X_i \leq s\}} - s \right| \geq (\epsilon_0 \delta)/4\right) \rightarrow 0, \end{aligned} \quad (28)$$

as $n \rightarrow \infty$. Combining (25) and (26), we can show (23) goes to 0 as $n \rightarrow \infty$. Similarly, (24) goes to 0 as $n \rightarrow \infty$. This gives us $\mathbb{P}(\sup_{s \in (\epsilon, 1-\epsilon)} |\mathcal{G}^*(s) - \hat{\mathcal{G}}^*(s)| \geq \epsilon_0) \rightarrow 0$ as $n \rightarrow \infty$, which completes the proof of Step 1.

Step 2. By Theorem 3.4, we have for any $\epsilon > 0$, $\sup_{s: d(s, s^*) > \epsilon} \mathcal{G}^*(s, c) < \mathcal{G}^*(s^*, c)$. Combining with $\sup_{s \in (\epsilon, 1-\epsilon)} |\mathcal{G}^*(s, c) - \hat{\mathcal{G}}^*(s, c)| \xrightarrow{P} 0$, we apply Theorem 5.7 of Van der Vaart (2000) and conclude $\hat{s} \xrightarrow{P} s^*$. \square

B.8. Mathematical details for Figure 1b and 1c

Imagine there are two final splitting nodes $\{t_1, t_2\}$ with the same mass of population. CART selects features $\{X_1, X_2\}$ for nodes $\{t_1, t_2\}$, respectively. The pdf of X_1 and X_2 in the $\{t_1, t_2\}$ are both uniform, respectively: $f_1(x) = 1$ and $f_2(x) = 1 \forall x \in [0, 1]$.

In node t_1 ,

$$P(Y = 1|X_1) =: \eta_1(X_1) = \begin{cases} 1, & \text{when } X_1 \in [0, \frac{1}{4}] \\ \frac{\sin(2\pi X_1) + 1}{2}, & \text{when } X_1 \in (\frac{1}{4}, \frac{3}{4}) \\ 0, & \text{when } X_1 \in [\frac{3}{4}, 1] \end{cases}$$

We depict $\eta_1(X_1)$ in Figure 1b. Since $\eta_1(X_1)$ is reflectional symmetric around $\eta_1(0.5)$, $s^{cart} = 0.5$. Splitting s^{cart} , policymakers target the left node $X_1 \leq 0.5$ only, the calculation is similar to Figure 1a in the introduction.

The unique optimal LPC solution is $s^* = \frac{5}{12}$. By shifting from s^{CART} to s^* , the policymaker excludes subpopulation $\{\frac{5}{12} < X_1 < \frac{1}{2}|t_1\}$ from the targeted group. Again, the mathematics is similar to Figure 1a in the introduction.

In node t_2 ,

$$P(Y = 1|X_2) =: \eta_2(X_2) = \frac{9}{11} X_2$$

The other node t_2 is depicted by Figure 1c. CART will split t_2 at $s^{CART} = 0.5$ because $\eta_2(X_2)$ is reflectional symmetric around $\eta_2(0.5)$. This would not target any subpopulations from t_2 , as both the left node mean and right node mean are

smaller than 0.75.

$$P(Y = 1|X_2 < 0.5) = \frac{\int_0^{0.5} \frac{9}{11} x dx}{0.5} = \frac{9}{44} < 0.75$$

$$P(Y = 1|X_2 > 0.5) = \frac{\int_{0.5}^1 \frac{9}{11} x dx}{0.5} = \frac{27}{44} < 0.75$$

On the other hand, the best split for LPC is $s^* = \frac{11}{12}$. This splits t_2 into two groups, the left node is entirely below the threshold whereas the right node is entirely above, as illustrated by the yellow and green segment in Figure 1c, respectively. As a result, splitting at s^* targets subpopulation $\{\frac{11}{12} < X_2 < 1|t_2\}$.

To summarize, splitting nodes t_1 and t_2 individually at s^{CART} versus s^* results in different target subpopulations:

- s^{CART} : Target $\{X_1 < \frac{1}{2}|t_1\}$.
- s^* : Target $\{X_1 < \frac{5}{12}|t_1\}$ and $\{\frac{11}{12} < X_2 < 1|t_2\}$.

Assuming that both t_1 and t_2 contain the same amount of population, the two sets of policies target the same proportion of the population, but $\eta(x, t_1) < 0.75$ for $x \in \{\frac{5}{12} < X_1 < \frac{1}{2}\}$, which is targeted by s^{CART} , whereas $\eta(x, t_2) > 0.75$ for $x \in \{\frac{11}{12} < X_2 < 1\}$, which is targeted by s^* . Therefore, policies based on LPC, i.e., s^* policy, target a **more vulnerable** subpopulation than policies based on observed Y classification, i.e., s^{CART} policy or CART/KD-CART policy. This idea appears in our diabetes empirical study, which we detail in Section 7.2.

C. Synthetic data simulation studies

C.1. Data generation processes

1. Generate features: $X_i \sim U(0, 1), i \in \{1, 2, 3, 4, 5\}$.
2.
 - **Ball**: $f(X) = \sum_{i=1}^3 X_i^2$.
 - **Friedman #1**: $f(X) = 10 \sin(\pi X_1 X_2) + 20(X_3 - 0.5)^2 + 10X_4 + 5X_5$
 - **Friedman #2**:
 - Make transformations: $Z_1 = 100X_1, Z_2 = 40\pi + 520\pi X_2, Z_4 = 10X_4 + 1$
 - Generate responses: $f(X) = \sqrt{Z_1^2 + (Z_2 X_3 - \frac{1}{Z_2 Z_4})^2}$.
 - **Friedman #3**:
 - Make transformations: $Z_1 = 100X_1, Z_2 = 40\pi + 520\pi X_2, Z_4 = 10X_4 + 1$
 - Generate responses: $f(X) = \arctan\left((Z_2 X_3 - \frac{1}{Z_2 Z_4})/Z_1\right)$.
 - **Poly #1**: $f(X) = 4X_1 + 3X_2^2 + 2X_3^3 + X_4^4$
 - **Poly #2**: $f(X) = X_1^4 + 2X_2^3 + 3X_3^2 + 4X_1$.
 - **Ring**: $f(X) = |\sum_{i=1}^3 X_i^2 - 1|$.
 - **Collinear**:
 - Create correlated features: $X_{i+3} = X_i + 0.1 \cdot \mathcal{N}(0, 1)$, where $i \in \{1, 2, 3\}$.
 - Generate responses: $f(X) = \sum_{i=1}^6 X_i$.
3. Map it to probabilities: $\eta = \text{Sigmoid}(f(X) - E(f(X)))$.
4. Generate labels: $y \sim \text{Bernoulli}(\eta)$.

C.2. CART, PFS, MDFS, wEFS, RF-CART, and RF-MDFS

Algorithm 1 Calculate_impurity

This function calculates sample impurity $\hat{\mathcal{G}}^{CART}$.

Input: x, y, x
 $y_l \leftarrow y[x \leq x], y_r \leftarrow y[x > x]$
 $\mathcal{G} \leftarrow \text{Var}(y_l) \frac{|y_l|}{n} + \text{Var}(y_r) \frac{|y_r|}{n}$
Output: \mathcal{G}

Algorithm 2 Calculate_distance

This function calculates the second term in (9) and $\hat{\mathcal{G}}^*$.

Input: x, y, x, c
 $y_l \leftarrow y[x \leq x], y_r \leftarrow y[x > x]$
 $\mathcal{G} \leftarrow (1 - |c - \bar{y}_l|) \frac{|y_l|}{n} + (1 - |c - \bar{y}_r|) \frac{|y_r|}{n}$
Output: \mathcal{G}

Algorithm 3 Calculate_weighted_risk

This function calculates sample loss function of wEFS.

Input: x, y, x, c
 $y_l \leftarrow y[x \leq x], y_r \leftarrow y[x > x]$
 $r_l \leftarrow |y_l[y_l > c]|, r_r \leftarrow |y_r[y_r > c]|$
 $\mathcal{R} \leftarrow (\mathbb{1}\{\bar{y}_l > c\}(|y_l| - r_l) + \mathbb{1}\{\bar{y}_r > c\}(|y_r| - r_r))c + (\mathbb{1}\{\bar{y}_l \leq c\}r_l + \mathbb{1}\{\bar{y}_r \leq c\}r_r)(1 - c)$
Output: \mathcal{R}

Algorithm 4 FindBestSplit

This function takes in data from the parent node and outputs the best feature, split point in terms of \mathcal{G}^{CART} .

Input: X, y
best_impurity, best_split, best_feature $\leftarrow 0, \text{None}, \text{None}$
for each feature x_i in X, i from 1 to p **do**
 sort X in terms of x_i
 for x in ordered samples in x_i **do**
 impurity \leftarrow Calculate_impurity(x_i, y, x)
 if impurity $<$ best_impurity **then**
 best_impurity \leftarrow impurity
 best_split $\leftarrow x$
 best_feature $\leftarrow i$
 end if
 end for
end for
Output: best_split, best_feature

Algorithm 5 Find_PFS_BestSplit

This function takes in data from the parent node and outputs the best feature, split point in terms of $\mathcal{G}^{PFS}(\lambda)$.

Input: $\mathbf{x}, \mathbf{y}, c, \lambda$
best_G_PFS, best_split $\leftarrow 0, \text{None}$
sort \mathbf{x}
for x in sorted \mathbf{x} **do**
 G_PFS $\leftarrow (1 - \lambda) \text{Calculate_impurity}(\mathbf{x}, \mathbf{y}, x) + \lambda \text{Calculate_distance}(\mathbf{x}, \mathbf{y}, x, c)$
 if G_PFS < best_G_PFS **then**
 best_G_PFS \leftarrow G_PFS
 best_split $\leftarrow x$
 end if
end for
Output: best_split

Algorithm 6 Find_wEFS_BestSplit

This function takes in data from the parent node and outputs the best feature, split point in terms of the weighted empirical risk.

Input: $\mathbf{x}, \mathbf{y}, c$
best_risk, best_split $\leftarrow 0, \text{None}$
sort \mathbf{x}
for x in sorted \mathbf{x} **do**
 risk $\leftarrow \text{Calculate_weighted_risk}(\mathbf{x}, \mathbf{y}, x, c)$
 if risk < best_risk **then**
 best_risk \leftarrow risk
 best_split $\leftarrow x$
 end if
end for
Output: best_split

Algorithm 7 Grow_Tree

Fit the tree-based model to (X, \mathbf{y}) when η or $\hat{\eta}$ is not provided.

Input: $X, \mathbf{y}, c, \text{current_depth}, \text{method}, \text{depth}, \text{min_samples}$
if $\text{current_depth} = \text{depth}$ **or** $n(\text{unique}(\mathbf{y})) = 1$ **or** $n(\mathbf{y}) < \text{min_samples}$ **then**
 Output: $\text{mean}(\mathbf{y})$
end if
 $\text{best_feature}, \text{best_split} \leftarrow \text{FindBestSplit}(X, \mathbf{y})$
 $\text{mask} \leftarrow (\mathbf{x}_{\text{best_feature}} < \text{best_split})$
 $\text{left_X}, \text{right_X} \leftarrow X[\text{mask}], X[!\text{mask}]$
 $\text{left_y}, \text{right_y} \leftarrow \mathbf{y}[\text{mask}], \mathbf{y}[!\text{mask}]$
if $\text{current_depth} = \text{depth} - 1$ **or** $\min\{n(\text{left_y}), n(\text{right_y})\} < \text{min_samples}$ **or** $\text{method} \neq \text{'CART'}$ **then**
 if $\text{method} = \text{'MDFS'}$ **then**
 $\text{new_best_split} \leftarrow \text{Find_PFS_BestSplit}(\mathbf{x}_{\text{best_feature}}, \mathbf{y}, c, 1)$
 else if $\text{method} = \text{'PFS'}$ **then**
 $\text{new_best_split} \leftarrow \text{Find_PFS_BestSplit}(\mathbf{x}_{\text{best_feature}}, \mathbf{y}, c, 0.1)$
 else if $\text{method} = \text{'wEFS'}$ **then**
 $\text{new_best_split} \leftarrow \text{Find_wEFS_BestSplit}(\mathbf{x}_{\text{best_feature}}, \mathbf{y}, c)$
 end if
 $\text{mask} \leftarrow (\mathbf{x}_{\text{best_feature}} < \text{new_best_split})$
 $\text{left_tree}, \text{right_tree} \leftarrow \text{mean}(\mathbf{y}[\text{mask}]), \text{mean}(\mathbf{y}[!\text{mask}])$
 Output: $\text{best_feature}, \text{new_best_split}, \text{left_tree}, \text{right_tree}$
else
 $\text{left_tree} = \text{Grow_Tree}(\text{left_X}, \text{left_y}, \text{current_depth} + 1, \text{method}, \text{depth}, \text{min_samples})$
 $\text{right_tree} = \text{Grow_Tree}(\text{right_X}, \text{right_y}, \text{current_depth} + 1, \text{method}, \text{depth}, \text{min_samples})$
 Output: $\text{best_feature}, \text{best_split}, \text{left_tree}, \text{right_tree}$
end if

Algorithm 8 Grow_Tree_wP

Fit the tree-based model to (X, \mathbf{y}) and $\hat{\eta}$ provided by Knowledge-Distillation.

Input: $X, \mathbf{y}, \mathbf{p}, c, \text{current_depth}, \text{method}, \text{depth}, \text{min_samples}$

if $\text{current_depth} = \text{depth}$ **or** $(\min(\mathbf{p}) > c$ **or** $\max(\mathbf{p}) < c$ **or** $n(\mathbf{y}) < \text{min_samples}$ **then**

Output: $\text{mean}(\mathbf{p})$

end if

$\text{best_feature}, \text{best_split} \leftarrow \text{FindBestSplit}(X, \mathbf{p})$

$\text{mask} \leftarrow (\mathbf{x}_{\text{best_feature}} < \text{best_split})$

$\text{left_X}, \text{right_X} \leftarrow X[\text{mask}], X[!\text{mask}]$

$\text{left_y}, \text{right_y} \leftarrow \mathbf{y}[\text{mask}], \mathbf{y}[!\text{mask}]$

$\text{left_p}, \text{right_p} \leftarrow \mathbf{p}[\text{mask}], \mathbf{p}[!\text{mask}]$

if $\text{current_depth} = \text{depth} - 1$ **or** $\min\{n(\text{left_p}), n(\text{right_p})\} < \text{min_samples}$ **or** $\text{method} \neq \text{'CART'}$ **then**

if $\text{method} = \text{'MDFS'}$ **then**

$\text{new_best_split} \leftarrow \text{Find_PFS_BestSplit}(\mathbf{x}_{\text{best_feature}}, \mathbf{y}, c, 1)$

else if $\text{method} = \text{'PFS'}$ **then**

$\text{new_best_split} \leftarrow \text{Find_PFS_BestSplit}(\mathbf{x}_{\text{best_feature}}, \mathbf{y}, c, 0.1)$

else if $\text{method} = \text{'wEFS'}$ **then**

$\text{new_best_split} \leftarrow \text{Find_wEFS_BestSplit}(\mathbf{x}_{\text{best_feature}}, \mathbf{p}, c)$

end if

$\text{mask} \leftarrow (\mathbf{x}_{\text{best_feature}} < \text{new_best_split})$

$\text{left_tree}, \text{right_tree} \leftarrow \text{mean}(\mathbf{p}[\text{mask}]), \text{mean}(\mathbf{p}[!\text{mask}])$

Output: $\text{best_feature}, \text{new_best_split}, \text{left_tree}, \text{right_tree}$

else

$\text{left_tree} = \text{Grow_Tree_P}(\text{left_X}, \text{left_y}, \text{left_p}, \text{current_depth} + 1, \text{method}, \text{depth}, \text{min_samples})$

$\text{right_tree} = \text{Grow_Tree_P}(\text{right_X}, \text{right_y}, \text{right_p}, \text{current_depth} + 1, \text{method}, \text{depth}, \text{min_samples})$

Output: $\text{best_feature}, \text{best_split}, \text{left_tree}, \text{right_tree}$

end if

C.3. Computational Complexity Analysis

Since our proposed algorithm only operates at the last split, the tree-building processes are identical in upper levels among 4 strategies. Next, we evaluate the computational complexity of the **final split**, i.e., split at the final level.

Suppose the sample size in a node at the second to last level is n and the number of features is p . In **CART**, the dominant step is to sort the samples based on each feature. With p features to consider, the computational complexity is $O(pN \log N)$. **PFS**, **MDFS**, and **wEFS** all determine the feature to split on using **CART**. The split point decision requires another $O(N)$ of time which is still dominated by the sorting process.

D. Additional empirical study: Forest fire

We use publicly available data from our empirical studies. The Pima Indian Diabetes dataset can be downloaded at <https://www.kaggle.com/datasets/uciml/pima-indians-diabetes-database>. The Montesinho Park forest fire dataset can be downloaded at <https://archive.ics.uci.edu/dataset/162/forest+fires>.

In this section, we use forest fire dataset to illustrate an application of our methods MDFS and RF-MDFS, and compare them to CART and RF-CART respectively.

The UCI Forest Fire dataset measures the characteristics of different forest fires in Montesinho Park with the response variable being the area burnt by a forest fire. We binarize the response by labeling those observations with a burnt area larger than 5 as 1, and 0 otherwise. 1 indicates a “big” forest fire. We search for conditions under which the probability of having a big forest fire is above $1/3$. We use the following features in the dataset for this task: X and Y-axis spatial coordinates, month, FFMFC, DMC, DC, ISI, temperature, RH (relative humidity), wind, and rain. All the acronyms except for RH are measures that positively correlate with the probability of a big forest fire. With a moderate sample size of 517, we set $m = 3$.

D.1. CART vs MDFS

As shown by Figure 2, the two sets of policies target many common groups except for the subgroup consisting of 43 observations defined by $FFMFC > 85.85$, $temp \leq 26.0$, $DC > 766.2$. This group that MDFS additionally targets has a 37.2% probability of catching a big forest fire, higher than the threshold. This finding aligns with Remark 5.2.

D.2. RF-CART vs RF-MDFS

As shown by Figure 2, RF-MDFS also additionally targets the subgroup consisting of 43 observations defined by $FFMFC > 85.85$, $temp \leq 26.0$, $DC > 766.2$. Hence, the comparison between RF-CART and RF-MDFS here also aligns with Remark 5.2.

Interestingly, both RF-CART and RF-MDFS (compared to CART and MDFS respectively) additionally target the subgroup $FFMFC > 85.85$, $temp > 26.0$, $RH \leq 24.5$.

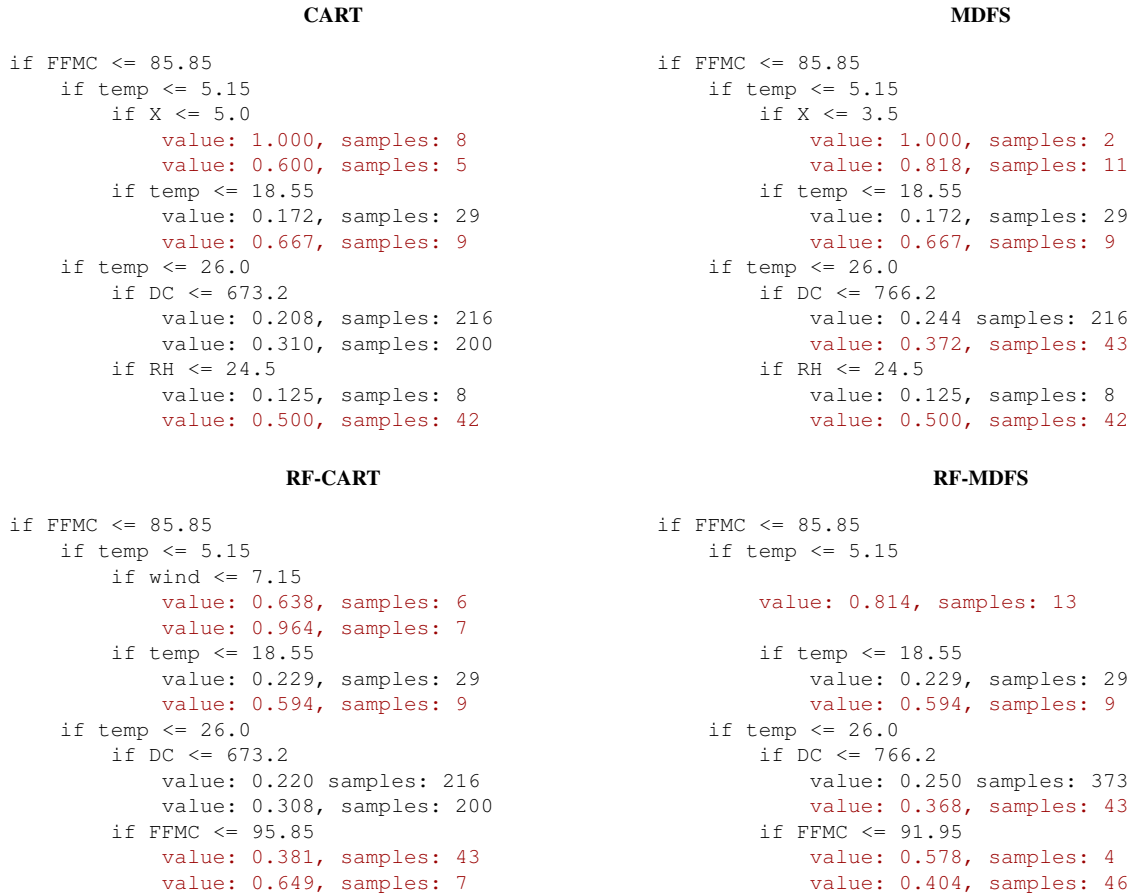


Figure 3. The targeting policies generated by CART, MDFS, RF-CART, RF-MDFS. The red groups are the targeted subpopulations predicted to have a higher than 1/3 probability of catching a big forest fire.